

## **Response to Interactive comments on: “Long-term Brown Carbon and Smoke Tracer Observations in Bogotá, Colombia: Association to Medium-Range Transport of Biomass Burning Plumes” by - Juan Manuel Rincón-Riveros et al.**

We thank the three anonymous reviewers for their thoughtful feedback, and constructive comments, which undoubtedly helped to improve our manuscript. The three reviewers accurately pointed out that the manuscript was missing an uncertainty analysis associated with the reported eBC and BrC concentrations, and they all emphasized the need to perform a sensitivity analysis for the parameters involved in the attribution of BrC and Black Carbon, to make the calculations more transparent. We addressed these issues (and all the other comments).

This particular issue was addressed in the following way:

- Detailed description showing step-by-step the decomposition of absorption measurements ( $b_{abs}$ ) due to fossil fuel (FF) and biomass burning (BB).
- Detailed discussion of uncertainties associated with our approach, both, from the decomposition into FF and BB (assumed angstrom exponents), and from uncertain values of mass absorption cross sections
- Sensitivity analysis to parameter choices.

All the additional comments were also addressed and incorporated in a new version of the manuscript. Detailed responses to each one of the reviewers' comments are detailed below (in blue) sorted by publishing date (Referee #1, Referee #3, and Referee #2). Referee comments are marked with **RC** and are in black. Author Responses are clearly labeled and are in blue.

### **Anonymous Referee #1**

Received and published: 30 January 2020

**RC:** Light-absorbing aerosols can affect both air quality and climate, so understanding their source and transport is important. This manuscript used a bunch of different observations to study the sources of light-absorbing aerosols over densely populated areas in the Central Andes of Northern South America. **It showed that these aerosols are closely related to medium-range transport of biomass burning plumes.** My comments are listed below.

Major comments

**RC:** I am concerned about the uncertainty associated with the BrC and BC measurements reported in this work. As mentioned in the work and reported by many other studies, there is large variability in reported mass absorption cross-section and Angstrom exponent values for absorbing aerosols. However, this study still used a single certain value for these variables (i.e.  $\tau=7.77 \text{ g/m}^3$ ;  $FF=1$ ;  $BB = 2$ ), without estimating the uncertainty due to the variation of these values. I expect that both eBC and BrC concentrations would change a lot if one assumes different values for these optical parameters. In addition, the authors should also estimate the uncertainties resulting from the process of measuring and analyzing the biomass burning tracers.

**Authors Response:** We have now addressed the issue of uncertainty by performing sensitivity analysis on the parameters used in the calculations. Regarding the use of a (mass absorption cross section)  $MAC 7.77 \text{ g/m}^2$  for eBC (at 880 nm), we would like to clarify that, by definition, it

is necessary to assume a specific MAC to convert  $b_{\text{abs}}$  into a “Equivalent Black Carbon” concentration. We strictly followed the recommendations of Petzold et al., 2013 (Atmos. Chem. Phys., 13, 8365–8379, 2013) by explicitly stating the MAC used, so the calculation is transparent and reproducible. We now explicitly mentioned this in the manuscript. Furthermore, we have now included  $b_{\text{abs}}$  in Figure 2 by adding a secondary axis.

One significant issue was the lack of sensitivity to parameters. **Figure R1** shows a sensitivity analysis performed on the parameters  $\alpha_{FF}$  and  $\alpha_{BB}$ . We computed the inferred BrC concentration for each set of parameters for high (DJF) and low (JJA) BB activity periods. Because our data is strongly influenced by urban emissions (dominated by traffic in Bogota) our observed Angstrom exponent is on average close to 1. Therefore, our deconvolution is much more sensitive to the assumed value of  $\alpha_{FF}$  than it is to the much more uncertain  $\alpha_{BB}$ . However, it should be noted that in all the parameter combinations the same trend remains, namely that during the high BB periods BrC is significantly higher than during JJA (i.e., has a strong seasonality). A discussion in this regard is now included in the manuscript and the sensitivity analysis included in the Supplementary Material.

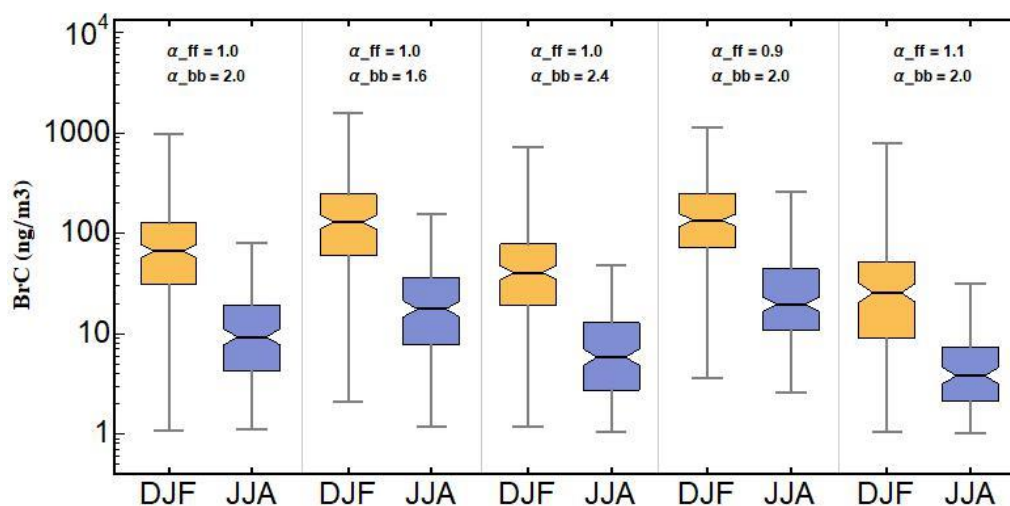


**Figure R1** – Response to Reviewers – Parametric sensitivity

Minor comments

**RC:** Line 168: “The quartz filters were pre-baked at 550°C for 12 hours to reduce their organic background and later placed in.” why is it needed to be heated? Wouldn’t it reduce the biomass burning semi-volatile OA?

**Authors Response:** The filters are pre-baked before being deployed for sampling. This is done exactly as the reviewer points out, to reduce semi-volatile OA from the filters, reducing this way any potential artifact during analysis post-sampling. We clarified this in the manuscript, and it reads “Previous to sampling, the quartz filters were pre-baked...”

**RC:** Line 174. What is LOD?

**Authors Response:** We intended LOD to stand for “Limit of Detection”. We now explicitly define the term in the manuscript.

**RC:** Line 173-179. It seems OC and EC are measured in the same way? Then how does one differentiate OC from EC?

**Authors Response:** OC and EC are measured in the same instrument, with a technique called TOT (thermal-optical transmittance). However, they are not measured in the same way. The TOT measurement is based on the fact that the organic carbon contained in particles volatilizes at different temperatures. The organic carbon is defined in this technique as the carbon that becomes gas in a Helium atmosphere at temperatures below 580°C. Meanwhile, EC in this technique is defined as the fraction of carbon that does not volatilize after exposing it to 580°C, but that oxidizes when oxygen is added to the controlled atmosphere at temperatures above 580°C. The quantification of carbon in each case (either volatilized or oxidized) is done by converting it to CH<sub>4</sub> to be detected with an FID.

We now expanded the explanation to avoid any potential confusion.

**RC:** Line 236. “The similarity between both datasets shows that eBC measurements at the site are overwhelmingly dominated by EC emissions from urban traffic and industrial emissions”. No absorbing OC emissions from urban traffic and industrial emissions?

**Authors Response:** The phrasing was modified in this section. The phrase now reads *“The strong correlation between both datasets suggests that eBC at the Monserrate site is closely associated to urban emissions. According to a recent emission inventory in Bogotá, mobile and industrial emissions are the dominant primary particle sources in the city. Furthermore, cargo and public transportation have the largest emissions share, and most of those vehicles are diesel powered (Pachón et al., 2018).”*

Regarding the question of -No absorbing OC from urban traffic and industrial emissions? - It is possible (as has been recently shown in the literature) that fossil fuels contribute to UV absorbing carbon (i.e., BrC). We acknowledge this in the paper now (in the introduction). However, EC is known to be the main absorber at near IR wavelengths, while OC from fossil fuel combustion is not a particularly strong absorber of near-IR light.

**RC:** Line 250. I think the major reason for the seasonal pattern in PM<sub>2.5</sub> is the different emission source/strength in different seasons.

**Authors Response:** Indeed, as the reviewer points out, this is exactly our working hypothesis in this paper, namely that biomass burning emissions in the region increase PM<sub>2.5</sub> concentration during the months of January-to-April, and we believe that we demonstrated that through measurements of biomass burning tracers in different seasons. In that specific paragraph we were merely pointing out that there are also meteorological conditions during those months (stronger surface inversions, stable conditions, lower mixing heights) that could concurrently have an impact of increasing PM<sub>2.5</sub> concentrations (this is explained in the reference Mendez-Espinosa et al., 2019). Furthermore, there is no clear annual pattern in either public transport, cargo transport, or industrial activities. There is no seasonal change in fuel composition as does occur in other countries.

**RC:** Line 263. I don't understand the reasoning here.

**Authors Response:** Point well taken. What we intended to say here was that the BrC we detected was likely aged biomass burning (because the sources are located hundreds of km away from our measurement site). The intended message is conveyed in the next section. Therefore, those lines were removed from the manuscript.

**RC:** Line 302. Not clear to me how the authors get these numbers.

**Authors Response:** These numbers were obtained by averaging WSOC for high and low BB activity seasons respectively (i.e, those represented by the open and filled circles in Figure 4b). This now reads: *“The mean WSOC observed for low BB activity was  $2.5\mu\text{gCm}^{-3}$  while for high-BB activity period was  $4.2\mu\text{gCm}^{-3}$  reaching up to  $8\mu\text{gCm}^{-3}$ .”*

### **Anonymous Referee #3**

Received and published: 5 February 2020

**RC:** This manuscript presents 3-year measurements of aerosol light absorption at multiple wavelengths over a site in the Northern South America (NSA) region. These measurements are combined with campaign-based biomass burning tracer measurements, MODIS fire counts and back-trajectory analysis to examine seasonal variations and source attributions of black carbon and brown carbon. **It is one of the few observational studies over NSA, and clearly demonstrates the influences of nearby biomass burning on the local air quality in densely populated areas. The long-term observations of biomass burning aerosol properties are also useful in revealing the regional and temporal variability in light absorbing aerosols. The sample collection and data postprocessing parts are well described.**

My major concern is about the inference of brown carbon concentration in section 2.2.

First, the assumptions of FF AAE (=1) and BB AAE (=2) are subject to large uncertainty. How sensitive are the derived BC and BrC concentrations to these assumed AAEs? It would be helpful to include some sensitivity analysis by varying the AAE values.

**Authors Response:** We have now included a sensitivity analysis showing how the uncertainties associated to these parameters impact the calculated attribution of absorption to combustion of biomass or fossil fuels (**Figure R1**). We also enhanced the discussion on the sources of uncertainty. In a now expanded supplementary material, we show the impact of parameter choice on the inferred BrC concentration. After performing this analysis, we showed the estimated BrC is only slightly affected by the choice of  $\alpha_{BB}$ , while it is more sensitive to  $\alpha_{FF}$ . However, in any case, the correlation of BrC and MODIS fire counts remains unchanged. Figure R1 and a subsequent discussion on the sensitivity is now included in the Supplementary Material.

For our specific data set, heavily influenced by traffic emissions, the observed angstrom exponent is closer to 1 ( $\alpha_{450\text{nm}-950\text{nm}} = 1.025 \pm 0.2$  and  $\alpha_{450\text{nm}-880\text{nm}} = 1.065 \pm 0.22$ ). Therefore, the inferred BB fraction is much more sensitive to  $\alpha_{FF}$  than it is to  $\alpha_{BB}$ . This can be seen in the **Figure R1** of this response (which has also been included in the Supplementary material for the final manuscript). This is positive for our study, as it is well known that  $\alpha_{BB}$  is

much more uncertain than  $\alpha_{FF}$  (which is largely accepted to be  $\approx 1$ ). This analysis is now included in the manuscript.

**RC:** Furthermore, lines 156-157 indicate that BrC concentration is computed as the product of eBC (equivalent BC concentration) and f\_BB (fractional contribution of biomass burning to absorption). This is confusing: isn't the product equal to BC concentrations from the BB sources? How is it related to the BrC concentration? Presumably, BB aerosols should include both BC and BrC. But the inference method of BrC in section 2.2 seems to imply that absorption in BB aerosols is due to BrC. The calculation of BrC concentrations needs clarification.

**Authors Response:** A section was included in the supplementary material to expand and clarify the decomposition method applied in our study. The Methods section was also expanded to improve clarity. The method we used (Sandradewi et al. 2008) is often referred to as the "Aethalometer model". In our manuscript (section 2.2), absorption at any given wavelength is indeed considered to be due both to BB and FF at any given wavelength. The FF contribution is associated with a  $\lambda^{-1}$  component (typical of BC rich FF sources) and the BB component is associated with an Angstrom exponent  $>1$  (typical of sources with light absorbing OC, such as BB). Our approach, as suggested by the manufacturer, is to use optical properties of black carbon to estimate mass. This is likely an underestimation of true BrC mass as most studies suggest its mass absorption cross sections is lower than that of BC.

**RC:** Another suggestion is since there are previous studies of BrC from the Amazon BB region, it'd be interesting to compare the derived BrC loadings and absorption properties over NSA with those in discussions. That would help extend the findings in this study to a larger regional context.

**Authors Response:** Done. We included some new references where absorption measurements of BB aerosols are made in NSA. These include (Saturno et al., ACP, 2018; Hamburguer et al, ACP, 2013). The addition now reads *"Our observations are broadly consistent with other available studies of aerosol absorption in the region that have reported an increase in  $b_{abs}$  and Angstrom exponent during the dry season. Observations at the ATTO tower in central Amazonia show  $b_{abs,635nm} = 4.0 \pm 2.2 Mm^{-1}$  during the dry season (Saturno et al., 2018). Other observations at Pico Espejo, in NSA show  $b_{abs,525nm} = 0.91 \pm 1.2 Mm^{-1}$  during dry season, corresponding to three times the mean value observed during the wet season. However, both sites correspond to locations near the source areas, while our observation site is an urban site far away from the main biomass burning areas"*.

Minor comments:

1. Line 38: the source of BrC is not limited to BB. They could also come from biofuel and biogenic sources. Suggest to revise the definition of BrC, i.e., Andreae and Gelencser, 2006

**Authors Response:** Point well taken. We rephrased and reorganized this section to acknowledge other sources of BrC. It now reads: *"The organic material (OM) present in aerosol particles, mainly those produced in BB, biofuel combustion, and from other sources, has been recently shown to absorb light in UV and short visible wavelengths more efficiently than BC. The absorption increases proportionally to the amount of OM present in the aerosol (Yan et al.,*

*2017; Mkoma et al., 2013). The collection of UV light-absorbing organic compounds present in aerosol particles is often termed Brown Carbon (BrC) (e.g., Kirchstetter et al., 2004; Andreae and Gelencsér, 2006; Wang et al., 2018), which is also a contributor to radiative forcing.”*

2. Lines 39-40: This sentence is inaccurate. The referred paper Bond et al., 2013 suggests that BC is the second largest contributors to anthropogenic radiative forcing, not BB particles

**Authors Response:** This oversight is now corrected in the manuscript. We now use the reference more accurately. It now reads: *“Due to its optical properties, EC is sometimes measured through light-absorption techniques, and when measured this way is referred to as equivalent Black Carbon (eBC) (Petzold et al., 2013). BC is the second largest contributor to anthropogenic radiative forcing with open burning of forests and savannas being the largest source (Stohl et al., 2015; Bond et al., 2013).”*

3. Line 65: missing a comma after “...their work”

**Authors Response:** Corrected.

4. line 66: replace “finding” with “indicating”

**Authors Response:** Corrected.

5. Line 83: “Levogucosan” doesn’t need an initial capital letter

**Authors Response:** Corrected.

Line 92: brown carbon and black carbon do not need initial letter capitalized. This needs to be corrected in other places as well

**Authors Response:** This is now corrected throughout the manuscript.

**RC:** Section 2.4: why not make the observatory site directly as the starting point of the back-trajectories, instead of Bogota? Since they are located at different altitudes.

**Authors Response:** The (lat, lon) coordinates used in the calculation are indeed those of the Monserrate site. This typo is now corrected. However, it should be noted that the spatial resolution of the meteorological data (1 degree, roughly equivalent to 110 km) is too coarse to accurately represent differences in back-trajectories starting from nearby points.

In a previous study, we found that due to the complex topography of the region, selecting starting points that are too close to or at the surface yields unrealistic back-trajectories. That is why we selected our arriving point at 1000 m.a.g.l, so it is not at the surface but remains within the mixing layer. This is now explicitly stated.

7. Line 123: W doesn’t need capitalization

**Authors Response:** Corrected.

8. Line 126: what is Davis Advantage Pro II?

**Authors Response:** This is now corrected. The Vantage-Pro2 (it was erroneously typed in the original manuscript) is the specific model of the meteorological station used for the data collection, which is made by Davis Instruments. This is now explicitly written in the manuscript.

9. Figure 1 (b): suggest to add a color scale for the background map. Is it for terrain height?

**Authors Response:** Point well taken. The figure was modified and included a more descriptive legend (See **Figure R2** included in this response). The color scheme is related to land-use cover (urban area, hills, and cropland/grassland). The shading is intended to qualitatively show terrain height variations, and this is mentioned in the caption. If height contour levels are included the plot gets cluttered and then is no longer effective.

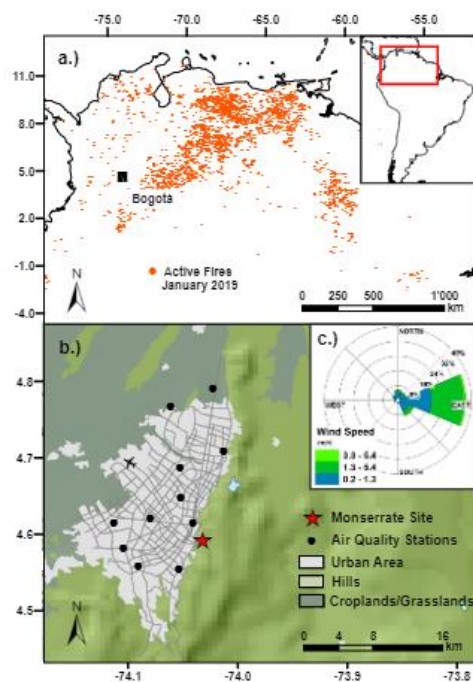


**Figure R2 – Response to Reviewers – Modified figure**

**RC:** Line 209: what is the spatial resolution of GDAS1 meteorology?

**Authors Response:** This is now corrected. GDAS1 meteorology is  $1^\circ \times 1^\circ$ . We now explicitly mention this in the manuscript.

## **Anonymous Referee #2**

Received and published: 26 February 2020

**RC:** This paper investigates the contribution of biomass burning from distant locations to air quality in Bogotá Colombia based on an extensive data set of aerosol light absorption at multiple wavelengths. Most data reported are from a measurement site upwind and at higher elevation than the city. Filter measurements of smoke tracers are also used to support the analysis, along with satellite-based fire counts and air mass back trajectories. **Overall the paper is a nice contribution to an understudied location and appropriate for publication in this journal. The results are interesting and the analysis very thorough**, however, some components are confusing and should be clarified.

I agree with the other two reviewers that the sensitivity of the reported results to the choice of AAE for BC (AAE=1) and for BrC (AAE=2) should be assessed. A value of BrC AAE of 2 seems especially

arbitrary. It is not clear to me why the authors utilized this analysis method at all since it adds unnecessary complexity and ambiguity; more related to this question follows below.

**Authors Response:** This comment is common to all reviewers. We addressed the issue of uncertainty in two ways: 1- By expanding and explaining the uncertainty associated to the attribution of absorption to BB and FF (including sensitivity analysis) and 2- by discussing potential uncertainties associated to transforming  $b_{\text{abs}}$  into eBC and BrC. Figures were modified to include an axis with  $b_{\text{abs}}$  (in  $\text{Mm}^{-1}$ )

We also expanded the supplementary material to clarify and make more transparent how the separation between BB and FF was performed.

**RC:** Why was 470 and 880 nm light absorption data used in the fractional biomass burning calculation? Explicitly state the reason. e.g, why not 370 and 950 nm, respectively? Similarly, why was 880 nm used for eBC, not 950 nm? Why not use all the wavelength data in some way, instead of just selecting a few wavelengths from the measurements (more on this below)?

**Authors Response:** We did not use data from the 370 nm channel since its noise to signal ratio is higher than that of other channels. To analyze BrC/BC typically a short wavelength and a near-IR wavelength are used. The choice of 880 nm for BC was done as this is what has been historically reported in previous aethalometer studies. BC at 880 and 950 nm channels is almost identical for our data.

This is now explicitly mentioned in the manuscript: *“The Angstrom exponent was computed using a wavelength in the near-UV, where absorption from some organic compounds can be significant, and a near IR wavelength, where absorption is dominated by black carbon. However, as the 370 nm channel had a larger noise to signal ratio, the limit of detection of this channel was considerably higher and was not used in the analysis. Equation 1 was then applied to  $b_{\text{abs}}$  measured at 470 nm and 880 nm wavelengths to compute an observed  $\alpha$ .”*

We also performed some sensitivity analysis on the pair of channels used to calculate the Angstrom exponent and evaluated its impact on our results. The mean Angstrom exponent varies slightly according to the wavelength pair chosen ( $\alpha_{450\text{nm}-950\text{nm}} = 1.025 \pm 0.2$  and  $\alpha_{450\text{nm}-880\text{nm}} = 1.065 \pm 0.22$ ) affecting the absolute value of inferred  $f_{\text{BB}}$  and BrC. However, because most of our analyses are based on correlations and associations to fires, these remain unchanged.

**RC:** Why does one even need to calculate a BC and BrC concentration, instead of just using the absorption coefficient? For example, simply using the absorption measured at a high wavelength as a tracer for BC and Abs measured at a low wavelength (e.g., 370, or if too noisy, 470 nm) as a tracer for BrC, after the Abs by BC at that wavelength is removed. This can be done by assuming a BC AAE of some value, such as 1. This seems like a much more transparent way to apportion BC and BrC from the multiwavelength Aeth data and it eliminates the need to assume a characteristic BrC AAE. It also simplifies an uncertainty analysis on the sensitivity of the results to only the value of BC AAE. It would be interesting to see a correlation between the BrC mass inferred by the method in this paper and the BrC abs at some wavelength (eg, 370 nm).

**Authors Response:** We are aware of the challenges of performing this decomposition. The method proposed by the reviewer is plausible, but it disregards contributions to absorption from BrC even at high wavelengths. The method we employed accounts for the contribution of BrC



and BC absorption at all wavelengths. We now discuss this much more thoroughly in the manuscript.

To address the valid concern regarding calculations of BC and BrC, we now added  $b_{\text{abs}}$  ( $\text{Mm}^{-1}$ ) in a secondary axis in Figure 2b and 2c. Since eBC and BrC are both proportional to  $b_{\text{abs}}$ , their correlation to the other datasets remains unchanged.

**RC:** Instead of picking a specific wavelength for BrC why not use all the Abs vs wavelength data. That is, fit the data with an AAE using all the wavelength and then use the fit to predict BrC AAE (data AAE-1) and then determine light absorption at some low wavelength with fit AAE-1.

**Authors Response:** During the data analysis phase, we did explore a variety of multi-wavelength methods. However, most of those methods require and even greater number of assumed parameters (e.g., Massabó et al., 2015). In their approach 5 wavelengths are used, but there is the need to assume three parameters and solve for three more. We tested this method and when applied to our data was much more sensitive to parameters choice than the simpler method we employed.

**RC:** Light absorption data are based on PM1, chemical composition and mass on PM2.5. PM1 was chosen to reduce possible influence of dust light absorption on the inferred BrC mass. The authors could test if there is any correlation between dust (eg, Ca2+) and BrC.

**Authors Response:** This is an excellent suggestion. However, we do not have Ca2+ data available in our samples. We think there is strong evidence showing that our BrC observations are strongly linearly correlated with levoglucosan and other BB tracers, suggesting its origin is indeed from biomass burning.

**RC:** Line 236-237: This line is unclear, suddenly there is a discussion that changes from eBC to EC. How does this data prove eBC is EC. Why not just say that eBC is from urban traffic and industrial emissions? Also, why is EC only assumed to be from these two sources?

**Authors Response:** Corrected. The phrase now reads *“The strong correlation between both datasets suggests that eBC at the Monserrate site is closely associated to urban emissions. According to a recent emission inventory in Bogotá, mobile and industrial emissions are the dominant primary particle sources in the city. Furthermore, cargo and public transportation have the largest emissions share, and most of those vehicles are diesel powered (Pachón et al., 2018).”*

**RC:** Line 248-249, first line after heading 3.1. This line is unclear. Is the eBC, BrC and fire counts data (Fig 3b) from the hill top site and the PM2.5 mass (Fig 3a) from the urban air quality stations in the city? That means that Fig 3a has data from two different sites? This complicates the comparison and the discussion that follows this line. More clarity is needed here. Please specify on the plots in Fig 3 what site the data is from.

**Authors Response:** This is correct. We tried to be as clear as possible in the caption and throughout the text. Now Figure 2 in the manuscript has been modified to include the origin of the data (i.e., panels (b) and (c) are marked Monserrate site). Similar changes were performed on Figure 3.

However, we want to emphasize to the reviewer that the aim of Figures 2 and 3 in the paper is to show that our BC measurements are strongly correlated to PM2.5 in the city, while BrC

measurements do not. Instead, BrC resemble regional fire counts according to their correlation coefficients.

**RC:** Line 282, typo change that to local emissions, to, than to local emissions.

**Authors Response:** Corrected.

**RC:** Line 289-290 states, ... However, optical methods are not always quantitative methods to determine BB aerosol loading. What is this statement based on?

**Authors Response:** The statement originally meant to refer to the issue of translating absorption coefficient data into concentrations (which, as the reviewer pointed out, require the assumption of a MAC). That is what we originally meant by “quantitative”. This whole paragraph is now rewritten and now reads: ***“However, due to the uncertainties in mass absorption cross sections, aerosol absorption measurements are not always straightforward to translate into BB aerosol concentrations. To establish the relationship between our Aethalometer based BrC (Section 2.2) and analytical methods to quantify BB aerosols (Section 2.3), we compared....”***

**RC:** Line 314. Is this true; the Monserrate site (also called at times, the hill top site) maybe a fairly close distance to the urban center, but it is decoupled from the city at times due to its higher elevation and changes in BL height. This mixing of the hill top site with the urban site throughout the paper leads to confusion. Often the term monitoring site is also use, which is apparently the Monserrate site, not the urban air quality sites? I suggest being more specific and consistent throughout the paper on what the sites are called.

**Authors Response:** Point is well taken. Our monitoring site is now referred to as [Monserrate Site](#) consistently throughout the whole manuscript. We also included a paragraph in the Methods to make explicit that our data comes from two different sources: our station at Monserrate (for eBC, BrC, and smoke tracers), and the AQ monitoring sites in the city (for PM<sub>2.5</sub> only).

**RC:** Last line of Conclusions. What is the 13% based on, mass ratio of eBC and BrC. This is then not an optical ratio and should be noted, it may also depend on how BrC was determined (AAE=2). Again, calculating mass concentrations of BC and BrC from the absorption data just leads to confusion and more uncertainty, in my view.

**Authors Response:** The 13% is based on  $f_{BB}$ . With the expanded and improved Methods and Supplementary materials we show that  $f_{BB} = b_{abs, BB}(\lambda)/b_{abs}(\lambda)$ . We performed a sensitivity analysis of this monthly mean  $f_{BB}$  with  $\alpha_{BB} = 2.0 \pm 0.4$  and  $\alpha_{FF} = 1.0 \pm 0.1$ . We now report a range in this percentage. It now reads: ***“During our observation period, the month with the largest contribution of BB aerosols to light-absorbing material was March with 10%±5%. The largest contribution was identified for February and March 2019, with 13%±6%. The uncertainty estimates in this fraction are due to uncertainty on the assumed absorption Angstrom exponent for biomass burning and fossil fuel burning used in the attribution algorithm”***

# Long-term Brown Carbon and Smoke Tracer Observations in Bogotá, Colombia: Association to Medium-Range Transport of Biomass Burning Plumes

Juan Manuel Rincón-Riveros<sup>1</sup>, Maria Alejandra Rincón-Caro<sup>1</sup>, Amy P. Sullivan<sup>2</sup>, Juan Felipe Mendez-Espinosa<sup>1</sup>, Luis Carlos Belalcazar<sup>3</sup>, Miguel Quirama Aguilar<sup>1</sup>, and Ricardo Morales Betancourt<sup>1</sup>

<sup>1</sup>Civil and Environmental Engineering Department, Universidad de los Andes, Bogotá, Colombia

<sup>2</sup>Department of Atmospheric Science, Colorado State University, Fort Collins, CO, USA

<sup>3</sup>Universidad Nacional de Colombia, Bogotá, Colombia

**Correspondence:** Ricardo Morales Betancourt (r.moralesb@uniandes.edu.co)

**Abstract.** Light-absorbing aerosols emitted during open biomass burning (BB) events such as wildfires and agricultural burns have a strong impact on the Earth's radiation budget through both direct and indirect effects. Additionally, BB aerosols and gas-phase emissions can substantially reduce air quality at local, regional, and global scales, negatively affecting human health. South America is one of largest contributors to BB emissions globally. After Amazonia, the BB emissions from the wildfires and agricultural burns in the grassland plains of Northern South America (NSA) are the most significant in the region. However, few studies have analyzed the potential impact of NSA BB emissions on regional air quality. Recent evidence suggests that seasonal variations in air quality in several major cities in NSA could be associated with open biomass burning emissions, but it is still uncertain to what those sources impact air quality in the region. In this work, we report on 3 years of continuous equivalent Black Carbon (eBC) and Brown Carbon (BrC) observations at a hill-top site located upwind of the city of Bogotá and we demonstrate its association with MODIS detected fires in a 3000 km x 2000 km domain. Off-line PM<sub>2.5</sub> filter samples collected during three field campaigns were analyzed to quantify water-soluble organic carbon (WSOC), organic and elemental carbon (OC/EC), and biomass burning tracers such as levoglucosan, galactosan, and potassium. MODIS Active Fire Data and HYSPLIT back-trajectories were used to identify potential biomass burning plumes transported to the city. We analyzed the relationship between BrC, WSOC, water-soluble potassium, and levoglucosan to identify signals of regional transport of BB aerosols. Our results confirm that regional biomass burning transport from wildfires occurs annually during the months of January and April. The seasonality of eBC followed closely that of PM<sub>2.5</sub> at the city air quality stations, however, the observed seasonality of BrC is distinctly different to that of eBC and strongly associated to regional fire counts. The strong correlation between BrC and regional fire counts was observed both at daily, weekly, and monthly time-scales. WSOC at the measurement site was observed to increase linearly with levoglucosan during high BB periods, and to remain constant at  $\sim 2.5 \mu\text{gC m}^{-3}$  during the low BB activity seasons. Our findings show, for the first time in this region, that aged BB plumes can regularly reach densely populated areas in the Central Andes of Northern South America. A source footprint analysis involving BrC

observations, back-trajectories, and remotely sensed fire activity shows that the eastern savannas in NSA are the main BB source region for the domain analyzed.

*Copyright statement.* TEXT

## 25 1 Introduction

Open biomass burning is a significant source of atmospheric aerosol particles and gas-phase pollutants (e.g., Bond et al., 2004; Aurell and Gullett, 2013; Tsimpidi et al., 2016). The particles emitted during biomass burning (BB) have a complex chemical composition dominated by primary organic matter (POM), elemental carbon (EC), and inorganic material such as sulfates, nitrates, and potassium (e.g., Yamasoe et al., 2000; Akagi et al., 2011). These species can contribute to deteriorated air quality levels in urban centers (e.g., Phuleria et al., 2005; Garcia-Hurtado et al., 2014; Kollanus et al., 2016). The impacts of BB plumes over air quality for sites located several thousand kilometers away from the BB sources has been demonstrated (e.g., Forster et al., 2001; Cottle et al., 2014). Many studies have documented the negative effects of BB emissions over human health (Youssouf et al., 2014; Haikerwal et al., 2015; Reid et al., 2016). Additionally, the ~~typically internally mixed~~ carbonaceous components of BB particles, which are typically internally mixed, contribute significantly to absorption of visible and UV light (Kirchstetter et al., 2004). ~~Due to its strong absorption of visible light, Elemental carbon is known to have a visible light absorption coefficient larger than that of any other aerosol component, and to substantially impact the radiation budget and climate. Due to its optical properties,~~ EC is sometimes measured through light-absorption techniques, and when measured this way is referred to as equivalent Black Carbon (eBC) (Petzold et al., 2013). ~~However, the BC is the second largest contributor to anthropogenic radiative forcing with open burning of forests and savannas being the largest source (Stohl et al., 2015; Bond et al., 2013). The organic material (OM) present in BB particles has a strong absorption aerosol particles, mainly those produced in BB, biofuel combustion, and from other sources, has been shown to absorb light in UV wavelengths, and this more efficiently than BC. The~~ absorption increases proportionally to the amount of OM present in the aerosol (Yan et al., 2017; Mkoma et al., 2013). The collection of UV light-absorbing organic compounds present in ~~BB particles are aerosol particles are often~~ termed Brown Carbon (BrC) (e.g., Kirchstetter et al., 2004; Wang et al., 2018). ~~Therefore, the aerosol particles emitted to the atmosphere through BB are the most significant short-lived climate pollutant and are the second largest contributors to anthropogenic radiative forcing (Stohl et al., 2015; Bond et al., 2013) (e.g., Kirchstetter et al., 2004; And~~, which is also a contributor to radiative forcing.

Biomass burning emissions from South America contribute the most to the global BC inventory, with 16% of the global emissions, surpassing those of other critical areas such as Asia and Africa (e.g., Koch et al., 2007; van der Werf et al., 2010). In particular, the Brazilian Amazonia and Cerrado regions produce substantial BB emissions, whose impacts have been the subject of numerous studies (e.g., Crutzen and Andreae, 1991; de Oliveira Alves et al., 2015; Gonçalves et al., 2016). Emissions from Amazonia and Cerrado occur typically between May and September, which corresponds to the dry season in the region

(Marengo et al., 2011). Fires in the savannas and tropical forests thousands of kilometers north of the Brazilian Amazonia, an area known as Northern South America (NSA), can also have significant global and local impacts (van der Werf et al., 2010).  
55 However, due to the significance of the BB emission from Amazonia, emissions from NSA have often been overlooked despite its potential impacts on air quality and climate (Thornhill et al., 2017). The equatorward location of NSA causes its annual precipitation and BB emissions patterns to differ strongly from those of Amazonia. Peak emissions in the former occur between January and April with minimum BB activity between June and October. Those BB activity patterns in NSA are mostly determined by the dynamics of wet and dry seasons, which are in turn controlled by the annual south-north migration of the In-  
60 ter-tropical Convergence Zone (ITCZ) (Pulwarty et al., 1998; Poveda et al., 2006; Mendez-Espinosa et al., 2019). Inter-annual variability in the intensity and length of the dry season, controlled by El Niño Southern Oscillation (ENSO), modulates the intensity of the peak BB emissions in NSA (Poveda et al., 2006).

The BB plumes generated in these fires can negatively impact the air quality experienced by over 60 million people that live, mostly in the urban areas, in Venezuela, Colombia, and Ecuador. Only recently some studies have focused on the air  
65 quality impacts of BB emissions in this region. Observational studies performed at *Pico Espejo* mountain (Venezuela), over 4000 m in altitude, detected the passage of BB plumes during the dry season (Hamburger et al., 2013). Because of its vertical elevation, the *Pico Espejo* site often sampled free-troposphere aerosols, showing the potential long-range transport of aged BB plumes (Schmeissner et al., 2011). More recently, PM<sub>2.5</sub> and ozone observations in the sparsely populated savannas in NSA showed extremely high concentrations even in small towns where measurements were performed (Hernandez et al., 2019).  
70 These high PM<sub>2.5</sub> and ozone levels were associated with distant fires in the Venezuelan savannas. The potential regional-scale air quality impacts of BB emissions in NSA was recently explored by (Mendez-Espinosa et al., 2019). In their work, a systematic analysis of air mass back-trajectories and MODIS hotspots for a ten-year period was conducted, [finding-indicating](#) a strong association between fire counts in NSA and PM<sub>2.5</sub> concentrations in cities located hundreds of kilometers from the BB sources. Mendez-Espinosa et al. (2019) showed that BB emissions from the NSA savannas could be transported westward  
75 impacting air quality in several large metropolitan areas. However, there were no direct measurements of BB available to confirm the presence of BB aerosols in the urban areas considered. Since the main BB source regions are located hundreds of kilometers from the most densely populated areas, the BB plumes are likely aged. Atmospheric aging of BB aerosols has been shown to increase the oxidative potential of the particles (e.g., Wong et al., 2019), potentially increasing the particles toxicity in addition to contributing to aerosol mass.

80 Detection of BB aerosols using chemical tracers is necessary to confirm the contribution of fires to aerosol loading at a given location. Traditionally potassium (K), levoglucosan, BrC, water-soluble organic carbon (WSOC), and other species have been used as biomass burning particle tracers (e.g., Sullivan and Weber, 2006a, b; Laskin et al., 2015; Shen et al., 2017; Martinsson et al., 2017). Potassium, *K*, has been extensively used as a BB tracer but there are significant non-biomass burning related sources of K, and it does not always correlate well with BB smoke (Pachón et al., 2013). Levoglucosan and other  
85 anhydrosugars, which are formed through the pyrolysis of cellulose, are more specific BB tracers (Simoneit et al., 1999). A potential limiting factor in the use of levoglucosan as a BB tracer is its oxidation in the atmosphere, with a lifetime of a few days when exposed to OH radical (Hennigan et al., 2010), reducing its abundance in long-range transported BB plumes

that have aged ~~substantially~~ in the atmosphere. Furthermore, Aerosol Mass Spectrometer data has shown that mass fractions associated with ~~Levoglucosan~~levoglucosan correlate strongly with light-absorbing carbonaceous material (e.g., Cubison et al., 2011; Lack et al., 2013). BB is also a significant primary source of WSOC (Sullivan and Weber, 2006b), but WSOC can also be formed through gas-to-particle conversion of gas-phase organics (e.g., Weber et al., 2007). WSOC has also been shown to be a strong absorber in the UV part of the spectrum, as indicated by measurements of absorption Angstrom exponent from filter extracts (Hecobian et al., 2010). Because of ~~the~~its optically active components, BB aerosols can be detected through multi-wavelength particle light absorption measurements (e.g., Jeong et al., 2004).

95 In this work, we determine for the first time, to our knowledge, the presence of BB plumes in a large metropolitan area in NSA by using long-term observations of BB tracers. We linked the smoke tracer observations with regional BB activity, showing the role of medium-range transport of BB plumes in urban air pollution in Northern South America. We approach this problem by carrying out measurements on a hill-top site ~~near~~in Bogotá, Colombia. Continuous ~~Brown Carbon and Black Carbon~~brown carbon and black carbon observations during a three-year period were used to establish temporal patterns in the BB tracer signal. The potential origin of the BB aerosols at the site was explored by analyzing the time series of MODIS active fire data in the NSA domain together with a systematic back-trajectory analysis (Mendez-Espinosa et al., 2019). Specific smoke tracers such as levoglucosan and water-soluble potassium were quantified. Our results show that smoke tracers in Bogotá are strongly associated with regional BB activity. The wildfires and agricultural burns in NSA from January to April contributes particularly to OC and WSOC concentration in the city of Bogotá.

## 105 2 Methods

We measured BrC and eBC continuously during a three year period at a hill-top site ~~located~~within the city limits in Bogotá, Colombia (Section 2.1). The site is known as the Monserrate site. Filter-based aerosol samples were also collected at ~~the~~this site over three different field campaigns spanning both, high and low BB activity in NSA. These samples were analyzed for smoke markers such as levoglucosan and other sugars. Water-soluble organic carbon (WSOC), inorganic ions, and EC/OC were also measured from ~~the~~these filter samples. Observations at our site were contrasted against those routinely collected at the Air Quality Monitoring Network of Bogotá (Section 2.5). Additionally, we combined MODIS active fire data with back-trajectory analysis to explore the potential transport of BB affected air masses by performing statistical association analysis between fire counts and smoke tracers concentrations (Section 2.4).

### 2.1 Measurement site description

115 The broader study domain covers a vast area of nearly 3.9 million km<sup>2</sup> (Figure 1a). The western part of NSA, dominated by the Andes mountain range, is a densely populated region with more than 60 million inhabitants. The eastern part of NSA includes the tropical grasslands and woodlands plains of the Orinoco river basin. The Orinoco river basin is sparsely populated and its economic activity is based on agricultural activities. The annual cycle of precipitation over the region is controlled by the meridional displacement of the ITCZ (Poveda et al., 2006). The ITZC southernmost location occurs typically during DJF.

120 These months, are therefore characterized by dryer weather in NSA as the deep convection areas are displaced southward, towards Amazonia (Mendez-Espinosa et al., 2019). This ~~mechanisms~~mechanism in turn, largely ~~explain the BB activity patterns~~explains the seasonality of BB activity in the region.

The measurement instruments were deployed at the *Monserate* Sanctuary (Long. = -74.05649°, Lat. = 4.60582°). This Sanctuary is located on a hill-top on the ~~Eastern~~eastern margin of the urban perimeter of Bogotá, Colombia (Figure 1b). The altitude of the *Monserate* site is 3152 m above sea level, and 550 m above the mean height of the Andean plateau where the city of Bogotá lies (Figure 1). Easterly winds prevail at the site, placing it upwind from the densely populated metropolitan area with 9 million people (Figure 1b). According to the Air Quality monitoring stations in the city, annual average PM<sub>2.5</sub> concentration was 19  $\mu\text{g m}^{-3}$  during 2018, with a strong seasonal cycle in which monthly-mean PM<sub>2.5</sub> between February and March can reach 35  $\mu\text{g m}^{-3}$  and decrease to 11  $\mu\text{g m}^{-3}$  in July. Primary aerosol emissions are estimated to be 2600 tons/year, with a ~~substantial~~large contribution from diesel powered public transport buses and cargo trucks (Pachón et al., 2018). Road dust re-suspension emissions are highly uncertain, but are thought to contribute significantly to primary emissions (Pachón et al., 2018). There are no significant emission sources or urbanized areas ~~West~~east of the city (Figure 1b). Therefore, the ~~measurement~~Monserate site location was intended to minimize the impact from the urban back-ground and allowing the detection of regional signals. Wind speed and direction, UV radiation, relative humidity, and barometric pressure were also recorded on-site with a frequency of 10 minutes (~~Davis Advantage Pro H~~using a meteorological station model Vantage-Pro2 (Davis Instruments, CA, USA.)).

## 2.2 BrC and BC measurements

Aerosol light absorption coefficient,  $b_{abs}$  ( $\text{Mm}^{-1}$ ), was measured continuously using a 7-wavelength (370, 470, 520, 590, 660, 880, 950 nm), Aethalometer (Aerosol inc., model AE-33) described by Drinovec et al. (2015). The measurements were carried out at the *Monserate* ~~Sanctuary~~ site during the three-year period from May 2016 ~~to~~ April 2019. Data was logged every 60 seconds. The sampling rate was 2 LPM through a PM<sub>1.0</sub> inlet (BGI model SCC0.732) to avoid potential mineral dust absorption interference on the measurements since most of either fresh or aged BB aerosol particles are in the sub-micrometer size range (Janháll et al., 2010). The  $b_{abs}$  raw data was corrected to account for filter loading effects (Virkkula et al., 2007). The loading correction parameter for each wavelength,  $k_\lambda$ , is automatically computed by the instrument by asymmetrically splitting the sample flow and simultaneously measuring attenuation at two differentially loaded filter spots (Drinovec et al., 2015). Absorption is also corrected for scattering using a multiple scattering parameter  $C = 1.57$ , i.e.,  $b_{abs} \rightarrow b_{abs}/C$ . Equivalent black carbon concentration, eBC ( $\mu\text{g m}^{-3}$ ), was computed from corrected  $b_{abs}$  measured at the 880 nm channel ~~using~~. This wavelength is customarily used in Aetholmeter measurements to define equivalent black carbon. At 880 nm the absorption from organics is minimized. Following the recommendations of Petzold et al. (2013), we report the mass absorption cross-section used to convert  $b_{abs}$  to eBC. We used a mass absorption cross-section  $\sigma = 7.77 \text{ m}^2\text{g}^{-1}$  ~~and a multiple scattering parameter  $C = 1.57$ , i.e.,  $\text{eBC} = b_{abs}/(C \times \sigma) = b_{abs}/\sigma$ .~~ The estimated eBC limit of detection was 40  $\text{ng m}^{-3}$  for a 1 hour interval. A lower limit of detection is achieved with longer integration periods.

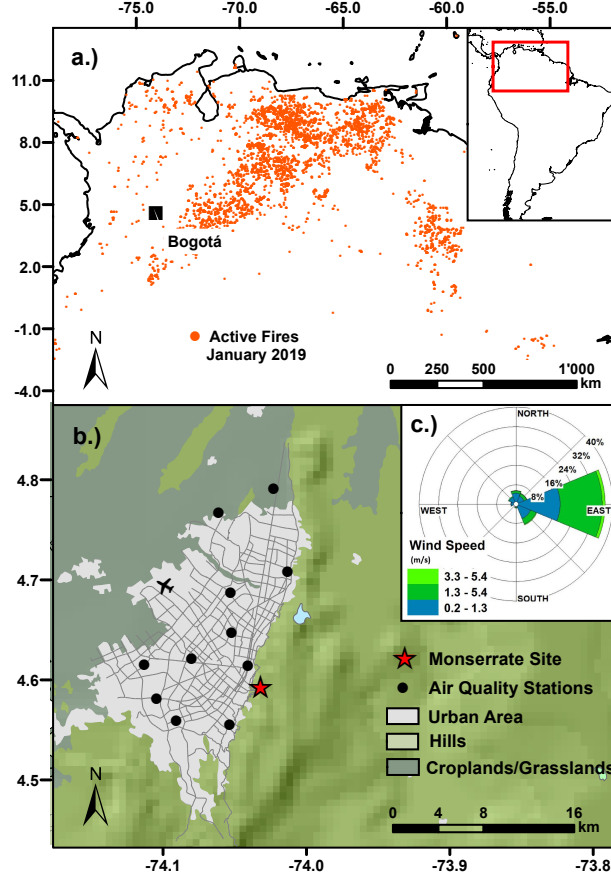


**Figure 1.** (a.) Geographic location of the Northern South America (NSA) domain as defined in this study and locations of MODIS hot-spots during January 2019. The inset shows the location of NSA relative to South America (b.) Location of the *Monserrate* Sanctuary site (star) near Bogotá and the AQ stations (filled circles). [Colors in the map indicate land-use type, and the shading is showing terrain height variations.](#) (c.) Wind direction observed at *Monserrate hill-top* site during the period May/2016 - Apr/2019

The spectral dependence of  $b_{abs}$  was characterized with the Angstrom Absorption Exponent,  $\alpha$ , which is the logarithmic slope of the relation between  $b_{abs}$  and wavelength,  $\lambda$ , i.e.,

$$155 \quad \frac{b_{abs}(\lambda_1)}{b_{abs}(\lambda_2)} = \left( \frac{\lambda_1}{\lambda_2} \right)^{-\alpha} \quad (1)$$

where  $b_{abs}(\lambda_i)$  is the absorption coefficient at wavelength  $\lambda_i$ . Several different methods to apportion absorption to either fossil fuels or biomass burning have been developed (e.g., Sandradewi et al., 2008; Massabò et al., 2015; Chen et al., 2018). In this work, deconvolution of  $b_{abs}$  between the contribution from fossil fuel and from biomass burning was done by applying the two-



component model described by Sandradewi et al. (2008). In their model, aerosol absorption at any given wavelength can be separated into the contribution of BB aerosol absorption and fossil fuels, i.e.,  $b_{abs}(\lambda) = b_{abs,BB}(\lambda) + b_{abs,FF}(\lambda)$ . Furthermore, it is assumed that the spectral dependence of absorption for each component is characterized by a specific Angstrom exponent. This is,  $b_{abs,BB} \sim \lambda^{\alpha_{BB}}$  and  $b_{abs,FF} \sim \lambda^{\alpha_{FF}}$ . ~~Many Observational studies suggest that  $\alpha_{FF} = 1$  (e.g., Lack and Langridge, 2013)  $\alpha_{FF} \approx 1$  (e.g., Sandradewi et al., 2008; Lack and Langridge, 2013), however, there is a large variability in published Angstrom exponent values associated to BrC (e.g., Hecobian et al., 2010; Harrison et al., 2013; Lack and Langridge, 2013). In this work we used  $\alpha_{FF} = 1$  and  $\alpha_{BB} = 2$  as has been suggested in several studies biomass burning aerosols (e.g., Hecobian et al., 2010; Harrison et al., 2010).~~

The Angstrom exponent was computed using a wavelength in the near-UV, where absorption from organic compounds can be significant, and a near IR wavelength, where absorption is dominated by black carbon. However, as the 370 nm channel had a larger noise to signal ratio, the limit of detection of this channel was considerably higher, and was not used in the analysis. Equation 1 was then applied to  $b_{abs}$  measured at 470 nm and 880 nm wavelengths to compute an observed  $\alpha$ . Sensitivity analysis were also carried out for  $\alpha$  calculated between the 470 nm and the 950 nm channel. The fraction of light-absorbing aerosol attributable to BB, i.e.,  $f_{BB}$ , is inferred from  $\alpha$  by applying the two-component model (Sandradewi et al., 2008), i.e.,

$$f_{BB} = \frac{1 - \frac{\lambda_1}{\lambda_2} 1 - \alpha_{FF}}{\frac{\lambda_1}{\lambda_2} 1 - \alpha_{FF}} \frac{\left(\frac{\lambda_1}{\lambda_2}\right)^{\alpha_{BB} - \alpha} - 1}{\left(\frac{\lambda_1}{\lambda_2}\right)^{\alpha_{BB} - \alpha_{FF}} - 1} \frac{b_{abs,BB}(\lambda_1)}{b_{abs}(\lambda_1)} = \frac{\left(\frac{\lambda_1}{\lambda_2}\right)^{\alpha - \alpha_{FF}} - 1}{\left(\frac{\lambda_1}{\lambda_2}\right)^{\alpha_{FF} - \alpha_{BB}} - 1} \quad (2)$$

A detailed derivation of Equation (2) can be found in the Supplementary Material. We assumed  $f_{BB}$  to be zero for  $\alpha \leq \alpha_{FF}$  and one for  $\alpha \geq \alpha_{BB}$ . ~~Brown Carbon concentration is then~~ Another method to apportion absorption to sources which uses 5 wavelengths was tested (Massabò et al., 2015). However, this method was found to be more sensitive to assumed parameters than the simpler Sandradewi et al. (2008) used here.

Since BrC absorption results from the contribution of many different compounds, quantifying BrC concentrations from absorption measurements is challenging, as there is no single mass absorption cross section that can be applied. BrC mass concentration was estimated here as the fraction of absorption that is attributable to BB, computed as  $BrC = eBC \times f_{BB}$ . This is likely an underestimation of BrC as their mass absorption cross section is lower than that of eBC. We used the parameters  $\alpha_{FF} = 1$ , as has been suggested in several studies, and assumed a central value of  $\alpha_{BB} = 2$ . However, as there is significant uncertainty in  $\alpha_{BB}$ , we performed a parameter sensitivity analyses by varying  $\alpha_{BB} = 2.0 \pm 0.4$  and  $\alpha_{FF} = 1.0 \pm 0.1$  (Sandradewi et al., 2008). The BrC estimates from optical absorption measurements are also compared with analytical quantification of levoglucosan and other BB combustion tracers (Section 2.3) known to be strongly related to BrC (Lack et al., 2013).

### 2.3 Biomass Burning Tracers

Filter-based aerosol samples were collected during three different field campaigns (Table 1) at the *Monserate* site described in Section 2.1. The campaigns were designed to span high and low BB activity periods in NSA. Two of these campaigns were

190 carried out during the high BB activity season (Campaigns 1 and 3) from January to April of 2018 and 2019, respectively, and  
one campaign was carried out during NSA rainy season (Campaign 2) from July to September 2018. Samples were collected  
onto 37 mm quartz filters for 24 hour periods (starting at midnight) every other day using a low-volume sampler. The sampler  
has a PM<sub>2.5</sub> inertial impaction stage and a sampling flow rate of 10 LPM. A total of 88 samples were collected and analyzed  
to quantify BB tracers on the aerosol samples. Blank samples at each sampling site were also analyzed. These handling blank  
195 filters were carried to the sampling site and placed in the sampling instrument with the vacuum pump turned off.

**Table 1.** PM<sub>2.5</sub> sampling campaigns carried out on *Montserrat* Site, where *N* stands for the number of filter samples

Campaign ID	Sampling Period	N
1. High-BB	2018/01/15 - 2019/04/15	31
2. Low-BB	2018/07/15 - 2019/09/15	24
3. High-BB	2019/01/15 - 2019/04/15	33

~~The~~ Prior to its deployment for sampling, the quartz filters were pre-baked at 550°C for 12 hours to reduce their organic  
background and later placed in a desiccator to prevent water vapor absorption. After sampling, the filters were stored in a freezer  
at -80°C in plastic Petri dishes. At the end of each field campaign samples were sent over-night in a refrigerated container for  
chemical analysis to the Collett Laboratory at Colorado State University.

200 Organic carbon (OC) and elemental carbon (EC) were determined from a 1.4 cm<sup>2</sup> punch in each filter using a thermal/optical  
transmission (TOT) EC/OC semi-continuous analyzer (Sunset Labs Inc.) following the NIOSH Method 5040 (Birch and Cary,  
1996). The ~~LOD~~ Limit of detection (LOD) was 0.2 µgCm<sup>-3</sup> and 0.5 µgCm<sup>-3</sup> for OC and EC, respectively. The remainder of  
the 37 mm filter was extracted in 15 ml of deionized water, and the extracts filtered with 0.2 µm PTFE syringe filter to remove  
insoluble particles. Water-soluble organic carbon (WSOC) was measured with a TOC analyzer (Siervers Model M9 Turbo).  
205 This instrument measures WSOC by converting all organic carbonaceous material in the water extract to carbon dioxide using  
chemical oxidation by ultraviolet light (UV) and ammonium persulfate. The LOD for WSOC in this study was 0.1 µgCm<sup>-3</sup>.  
The overall measurement uncertainties for compounds analyzed is estimated to be ~ 10% (Sullivan et al., 2008).

A fraction of the aqueous extract was used to analyze for carbohydrates (including levoglucosan) through High-Performance  
Anion-Exchange Chromatography with Pulsed Amperometric Detection (HPAEC-PAD) (Sullivan et al., 2011). This technique  
210 uses a Dionex DX-500 series ion chromatograph with a Dionex GP-50 pump and a Dionex ED-50 electrochemical detector  
operating in integrating amperometric mode using waveform A. Detailed descriptions of this method can be found elsewhere  
(e.g., Sullivan et al., 2008, 2011). The LOD for carbohydrates quantification is less than ~ 0.1 ng/m<sup>3</sup>.

Another portion of the aqueous extract was used to quantify inorganic anions and cations, including water-soluble potassium  
(WSK). For this analysis we used a Dionex ICS-3000 ion chromatograph with a conductivity detector, a isocratic pump and self-  
215 regenerating cation/anion suppressor. Cations were separated using a Dionex IonPac CS12A analytical column with a flowrate  
at 0.5 mL min<sup>-1</sup> of 20 mM methanesulfonic acid eluent. The LOD for the various cations was 0.02 µg m<sup>-3</sup>. In the case of  
anions, a Dionex IonPac AS11-HC anion-exchange column with a flowrate at 1.5 mL min<sup>-1</sup> of sodium hydroxide eluent was

employed. The LOD for anions was  $0.01 \mu\text{g m}^{-3}$ . This type of method has been applied by other studies (Tzompa-Sosa et al., 2016; Prenni et al., 2012) and further method details are presented by Sullivan et al. (2008).

## 220 2.4 Active Fires and Back-trajectory Analysis

MODerate-resolution Imaging Spectroradiometer (MODIS) observations were used to locate and count fires and its Fire Radiative Power (FRP) daily in the NSA domain (long. $=-79.0^\circ$ , lat. $=-4.4^\circ$  as bottom left; long. $=-51.7^\circ$ , lat. $=13.1^\circ$  as top right) during May 2016 to April 2019. Only those active fires labeled with a  $\geq 75\%$  confidence level were included in the analysis (Justice et al., 2002). The spatial distribution of fires during January 2019 is shown in Figure 1a, where the substantial  
225 dry-season BB activity on the eastern savannas of the Orinoco river basin can be seen.

We constructed several time series of daily fire counts,  $N_f$ , in the NSA domain by applying a variety of criteria. In the simplest criterion, all active fire counts in the domain,  $N_{f_{All}}$ , with confidence  $\geq 75\%$  were considered. Next, a set of distance criteria were applied and only the subset  $N_{f,<R}$  of fire counts within a circular region with radius  $R$  from Bogotá were included. Time series considering radii of 200 km, 400 km, 600 km, 1000 km, and 1500 km were built following this method. Similarly,  
230 additional time series of only those fires in an annular region,  $N_{f,R_1-R_2}$ , defined by distances  $R_1$  and  $R_2$  were considered, i.e., those fires within  $R_1 < R < R_2$ .

MODIS active fire data was combined with Lagrangian back-trajectory analysis to explore the potential transport of BB affected air masses following the methods of Mendez-Espinosa et al. (2019). Air-mass back trajectories arriving with three hour intervals (00:00, 03:00, 06:00, 09:00, 12:00, 15:00, 18:00 and 21:00 GMT-5) at [Bogotá-the Monserrate site](#) at 1000 m a.g.l., i.e.,  
235 eighth daily, were computed using the NOAA HYSPLIT model (Stein et al., 2015; Draxler and Hess, 1998; Donnelly et al., 2015). Each trajectory was calculated for 96 hours prior to arrival in order to account for distant emission sources and avoid uncertainties on regional analysis due to longer trajectories (Donnelly et al., 2015). The Lagrangian trajectories were driven by GDAS1 meteorological fields [which have an horizontal resolution of  \$1^\circ \times 1^\circ\$](#)  (Su et al., 2015). The trajectory data was systematically analyzed using the OpenAir package (Carslaw and Ropkins, 2012) and the SplitR package of the open source  
240 programming language R. With this method, we constructed a time series of up-wind fire counts,  $N_{f_{upW}}$ , using an algorithm to select only upwind fires according to the trajectory analysis (Mendez-Espinosa et al., 2019). For this, a buffer zone of 150 km was defined around each of the 96 hourly locations defining one of the eight back-trajectories reaching the receptor city in any given day. Then, only active fires in these buffer zones were included in the analysis. This method should account for any time lag between the occurrence of a fire and the effect over concentrations at a distant site. Additionally, time series of daily  
245 FRP data were constructed following the same procedures described here for  $N_f$ . A statistical association analysis was then carried out between the data collected on-site, and the time series of fire counts and FRP. A source-footprint analysis was performed by combining the BrC observations, back-trajectories, and MODIS retrieved FRP (Supplementary Material).

## 2.5 $\text{PM}_{2.5}$ and eBC from the city monitoring stations

We retrieved  $\text{PM}_{2.5}$  ~~and eBC~~ concentrations from the public air quality monitoring data repository of the Air Quality Monitoring Network of Bogotá. The air quality network data was ~~then~~ used to contrast ~~the~~ [their](#) magnitude and temporal patterns ~~of~~  
250

~~the measurements to those of the eBC and BrC observations at the Monserrate Sanctuary site to those at the city site.~~ The  $PM_{2.5}$  record from the air quality network covers the entire monitoring period ~~but the eBC data covers only the last 9 months, since Aethalometers started operating on September of 2018.~~ The air quality network has eleven stations across the city ~~with 6 of those currently monitoring eBC~~ (Figure 1).

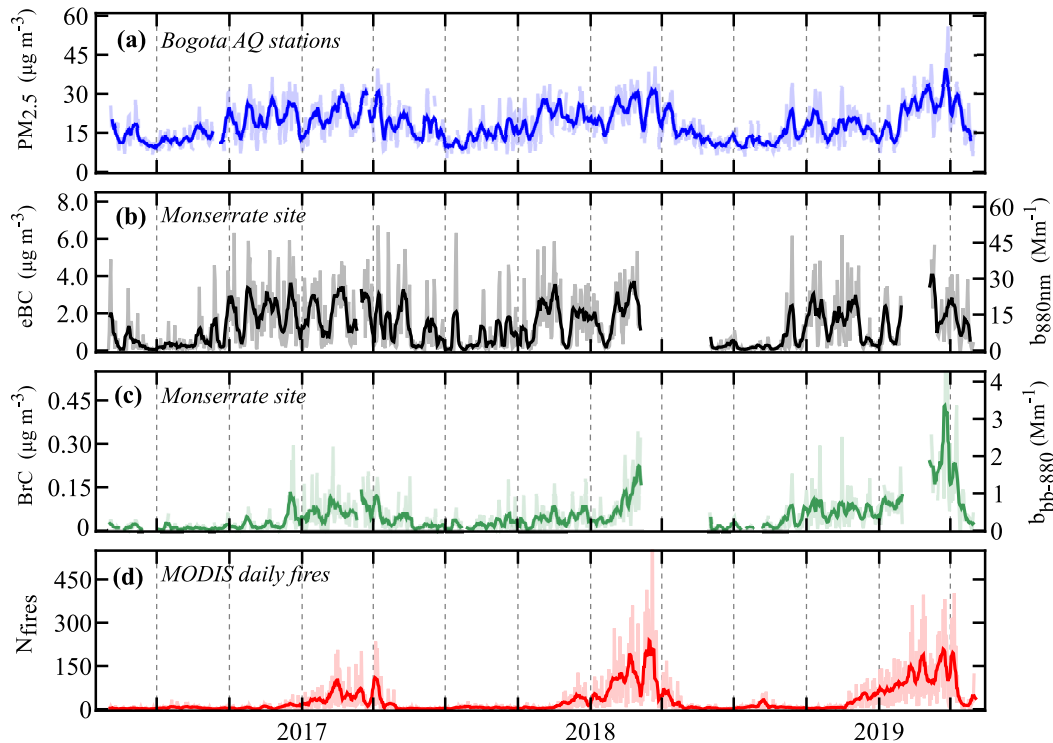
### 255 3 Results and Discussion

~~Equation 2 was applied~~ Multi-wavelength observations of  $b_{abs}$  were used to apply Equation 2 as described in Section 2.2 to obtain eBC, absorption Angstrom exponent,  $f_{BB}$ , ~~and BrC,~~  $b_{abs, BB}$  (at 470 and 880 nm), and the corresponding estimated BrC, all with hourly and daily temporal resolution. The complete time-series of daily-mean observations of eBC and BrC at the ~~hill-top Monserrate~~ site can be seen in Figure 2. Two short maintenance and calibration periods are seen in the data set as missing values. ~~Observed~~ Mean total aerosol absorption  $b_{abs}$  at 880nm for the observation period was  $11.8 \pm 11.2 Mm^{-1}$ . The large variability in the data occurs both at daily and monthly time scales. There is a marked seasonal cycle, with mean  $b_{abs} = 15.0 Mm^{-1}$  for January to March (JFM) and  $5.0 Mm^{-1}$  for June to August (JJA). Similarly, the mean absorption attributable to BB,  $b_{abs, BB}(470nm)$ , for the entire campaign was  $2.41 \pm 2.87 Mm^{-1}$ , with a statistically significant difference between the high BB burning activity periods (JFM) and those of low BB activity (JJA). The JFM  $b_{abs, BB}(470nm)$  was  $4.05$   
265  $Mm^{-1}$  while the JJA mean was  $0.71 Mm^{-1}$ .

Accordingly, the observed daily-mean eBC concentration (Figure 2b) ranged from 0.02 to  $5.0 \mu g m^{-3}$ . Inferred BrC concentration were lower, with a maximum daily-mean of  $0.44 \mu g m^{-3}$ . ~~During~~ The highest  $f_{BB}$  was detected during the 2018-2019 dry season (DJF) ~~the highest  $f_{BB}$  was detected at the site,~~ reaching up to ~~13% for the monthly mean for December and January,~~ a monthly mean of 15% for February. The campaign mean absorption Angstrom exponent was close to 1, indicating a strong influence from fossil fuel combustion sources. Observed  $\alpha$  was found to vary according to the wavelength pair chosen in its calculation, i.e.,  $\alpha_{450nm-950nm} = 1.025 \pm 0.2$  and  $\alpha_{450nm-880nm} = 1.065 \pm 0.22$ . A sensitivity analysis on the  $b_{abs, BB}(470nm)$  depending on the specific wavelengths chosen to calculate absorption Angstrom exponent are included in the Supplementary Material. Additionally, daily-mean  $PM_{2.5}$  retrieved from the AQ monitoring stations is shown in Figure 2a, and  $N_{f,600-1000}$  constructed according to Section 2.4 is shown in Figure 2d.

275 Day to day variations in  $PM_{2.5}$  ~~and eBC measured at the AQ monitoring network and eBC observed~~ at the Monserrate Site site have a similar temporal pattern (Figure 2a and 2b). A simple linear correlation analysis ~~using the Spearman correlation~~ between the two data sets ~~using the Spearman correlation,~~  $\rho_{PM_{2.5}, BC}$ , confirms this relationship as  $\rho_{PM_{2.5}, BC} = 0.76$ . The ~~similarity high correlation~~ between both datasets ~~shows that eBC measurements at the site are overwhelmingly dominated by EC emissions from urban traffic,~~ suggests that eBC at the Monserrate site is closely associated to urban emissions. According to  
280 a recent emission inventory in Bogotá, mobile and industrial emissions ~~are the dominant primary particle sources in the city.~~ Furthermore, cargo and public transportation have the largest emissions share, and most of those vehicles are diesel powered (Pachón et al., 2018). To examine the degree of influence of the city emissions at the ~~measurement Monserrate~~ site we analyzed mixed layer height from daily radiosondes data at the airport station (SKBO station). We found that the Monserrate

**Figure 2.** Time series of (a.)  $\text{PM}_{2.5}$  ( $\mu\text{g m}^{-3}$ ) from Bogotá Air Quality Monitoring Stations, (b.) equivalent Black Carbon ( $\mu\text{g m}^{-3}$ ) from Monserrate Site (left axis is  $b_{\text{abs},880\text{nm}}$  in ( $\text{Mm}^{-1}$ )), (c.) Brown carbon ( $\mu\text{g m}^{-3}$ ) from Monserrate Site (left axis is  $b_{\text{bb},880\text{nm}}$  in ( $\text{Mm}^{-1}$ )), and (d.) Daily MODIS active fire counts in NSA within 600 km and 1000 km from Bogotá. Thick lines are seven-day moving averages from the original time series of daily-mean values. Faded lines in all panels show daily-mean values.



site is typically above the mixed layer early in the morning, up until 9:30 am when the mixing layer expands surpassing the  
 285 site altitude (Supplementary Material). Diurnal concentration patterns for eBC at the Monserrate Site and at the air quality  
 monitoring stations support this hypothesis, since morning peak concentrations are observed with a lag of 1.5 to 2 hours at  
 Monserrate [site](#) compared to the city AQ stations (Supplementary Material).

**In-contrast, BrC data** Contrastingly, the BrC observations in Figure 2 **has show** a significantly different temporal structure  
 compared to both  $\text{PM}_{2.5}$  and eBC. A correlation analysis shows a substantially lower correlation,  $\rho_{\text{PM}_{2.5}, \text{BrC}} = 0.54$ , compared  
 290 to that of eBC and  $\text{PM}_{2.5}$ . This **difference in dissimilarity in the observed** temporal patterns is indicative of a difference in the  
 activity of sources of BrC and those of eBC, **possibly** suggesting that the BrC signal is controlled by BB outside of the city.

### 3.1 Monthly-mean BrC and eBC

The annual cycle observed for eBC at the Monserrate **hill-top** site (Figure 3**ab**) is similar to that of  $\text{PM}_{2.5}$  **from-registered**  
**at** the air quality **stations-monitoring stations within the city** (Figure 3**ba**), with a bi-modal concentration pattern exhibiting

295 maxima from February to March and from October to November. This Part of the seasonal pattern in  $PM_{2.5}$  is in part has been previously explained by higher mixing heights during JJA and by lower mixing heights and increased static stability from December to March (Mendez-Espinosa et al., 2019). Monthly mean eBC at the Monserrate Site site ranges from  $0.25 \mu g m^{-3}$  in July to  $1.70 \mu g m^{-3}$  during February and November. Consistent with what is observed at a daily time-scale, the similarity between the annual eBC and  $PM_{2.5}$  variations is expected as the site is within the urban mixed layer during most of the day and therefore, heavily impacted by urban traffic emissions. Contrastingly, BrC seasonality at the Monserrate site is distinctly different from that of either eBC or  $PM_{2.5}$ , with a lone maximum from February to April and not exhibiting a second peak in the last months of the year (Figure 3b). This discrepancy between the seasonal cycles of ~~BC and BrC further eBC and BrC strongly~~ suggest that sources of both types of light-absorbing particles have different activity patterns along the year. Since eBC seems to be related to local emissions, the sources of BrC must be of a different type.

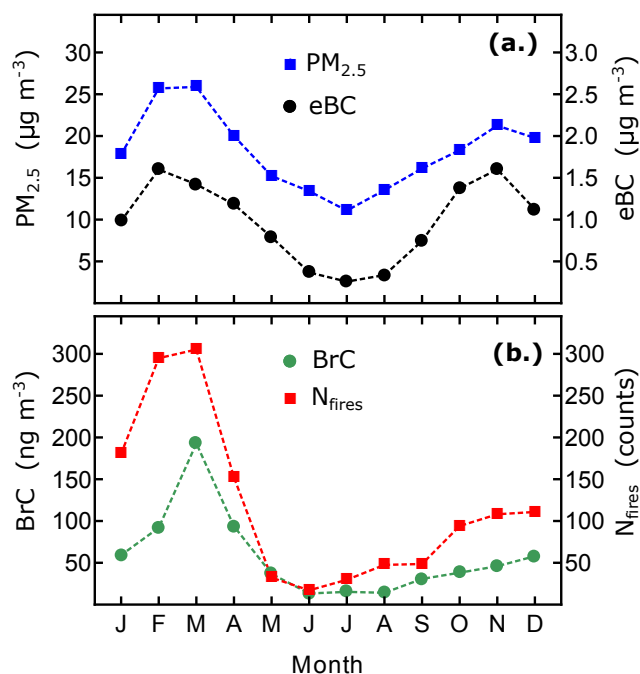


**Figure 3.** Monthly mean time series of Bogotá's  $PM_{2.5}$  ( $\mu g m^{-3}$ ), equivalent Black Carbon ( $\mu g m^{-3}$ ), ~~Brown Carbon brown carbon~~ ( $\mu g m^{-3}$ ) and fire counts. ~~The number of fire counts~~ BrC and eBC are measured at the Monserrate site, while the  $PM_{2.5}$  are observations from the air quality monitoring network.  $N_f$  is the monthly mean of daily fire counts.

305 A potential explanation for the distinct seasonality of BrC at the site is found when analyzing the BB activity through MODIS active fire data after applying the fire counting algorithms described in Section 2.4. Figure 3b shows that the seasonality of BB activity is similar to that observed for BrC at the site, further suggesting a potential association between ~~BB tracers in the city~~ BrC measured in the Monserrate site and regional BB activity.

310 ~~The distance of the most intense BB source areas in the eastern savannas and south-eastern tropical forests to the measurement site implies that the detected BB signal is due to aged biomass burning aerosols. This is supported by the high correlation with regional fire counts but the relatively low BrC concentration observed on site. The systematic increase in BrC during the first months of the year suggests that this is due to an increase in the contribution of BB aerosols to the regional background, rather than to sporadic episodes of high BB loading caused by transport of intense plumes.~~ Our observations are broadly consistent with other available studies of aerosol absorption in the region that have reported an increase in  $b_{abs}$  and Angstrom exponent during the dry season. Observations at the ATTO tower in central Amazonia show  $b_{abs,635nm} = 4.0 \pm 2.2 \text{ Mm}^{-1}$  during the dry season (Saturno et al., 2018). Other observations at Pico Espejo, in NSA show  $b_{abs,525nm} = 0.91 \pm 1.2 \text{ Mm}^{-1}$  during dry season, corresponding to three times the mean value observed during the wet season. However, both sites correspond to locations near the source areas, while our observation site is an urban site far away from the main biomass burning areas.

### 3.2 Association with MODIS fire counts

320 To establish whether observed BrC at the ~~Monserrate Site~~ Monserrate site is related to regional BB activity, we performed a systematic statistical association analysis between BrC observations and the different fire counting methods described in Section 2.4. The Spearman correlation for the daily-mean as well as the seven-day moving average for eBC and BrC with  $N_f$  were calculated and summarized in Table 2. Overall, a weak statistical association was found between eBC and  $N_f$ , with values much lower than those observed between eBC and  $\text{PM}_{2.5}$ , confirming that a large fraction of eBC measured at  
 325 the site is likely from local fossil fuel combustion sources. Furthermore, regardless of the fire counting scheme applied, the statistical association between BrC and  $N_f$  is stronger in all cases than that of eBC and  $N_f$ . Thus, despite the proximity of the measurement site to the city and the impact of local emissions, the association between regional BB activity in NSA and BrC suggest that the measurements at the site are able to differentiate the relatively small signal from regional BB to that of local emissions.

**Table 2.** Statistical association expressed through Spearman correlation between the different fire counting methods and eBC and BrC measured at Monserrate Site. Mov. Avg. is the Spearman correlation between smoothed time series with a seven-day moving average, and Daily are the Spearman correlations between daily-mean variables

MODIS fire counts	BrC		eBC	
	Mov. Avg.	Daily	Mov. Avg.	Daily
$600 < R < 1000 \text{ km}$	0.570	0.443	0.133	0.168
$400 < R < 600 \text{ km}$	0.556	0.368	0.195	0.170
$R < 1000 \text{ km}$	0.554	0.448	0.148	0.186
All-fires (>75%)	0.545	0.419	0.263	0.214
$R < 600 \text{ km}$	0.521	0.369	0.167	0.163
$200 < R < 400$	0.495	0.334	0.171	0.178
$1000 < R < 1500$	0.454	0.251	0.095	0.035
Up-Wind fires	0.454	0.352	-0.063	-0.031
$R < 400 \text{ km}$	0.453	0.316	0.114	0.152
$R < 200 \text{ km}$	0.173	0.107	-0.096	0.005

330 Table 2 is ~~ordered~~sorted according to the Spearman correlation between the seven-day moving average fire counts and BrC. The result of the analysis shows a stronger association between BrC and distant fires, and the weakest association for those fires within 200 km of Bogotá. This is likely due to the substantially lower number of nearby fires compared to the abundant hot-spots in the Orinoco savannas and tropical forests. Therefore, either at a daily or weekly time-scales, the concentration of UV absorbing carbonaceous material in Bogotá is more closely associated with regional BB activity ~~that~~than with local emissions. The potentially more accurate fire counting method that only includes up-wind fires does not perform much better than the other methods considered. ~~This result supports the idea that there is~~ These results are consistent with an increase in the regional BB aerosol background ~~, decreasing the relative importance of direct advection of BB plumes during the dry season.~~ A spatial footprint analysis of BB source areas shows that in the period from December to March, the Orinoco savannas are ~~likely~~ the the likely source regions impacting BrC at the Monserrate measurement site (see Supplementary Material). The travel time of the air masses from the savannas to the measurement site suggests that ageing of the organic aerosols can occur.

### 3.3 Brown Carbon and Smoke Tracers

The continuous BrC measurements described in Section 3.1 are a strong indicator of the enhanced presence of UV absorbing aerosols. However, ~~optical methods are not always quantitative methods to determine BB aerosol loading due to the uncertainties in mass absorption cross sections, aerosol absorption measurements alone are not straightforward to translate into BB aerosol concentrations.~~ To establish the relationship between ~~BrC and BB aerosols~~ the Aethalometer based BrC (Section 2.2) and analytical methods to quantify BB aerosols (Section 2.3), we compared ~~the~~ 24-hour average BrC ~~concentration with the concentration of~~ concentrations with smoke markers levoglucosan, galactosan, WSK, and WSOC, as well as EC. The analysis was done for those specific dates where collocated filter-based samples and optical BrC observations were available, totalling 58 valid dates. A strong linear association was found between BrC and levoglucosan ( $R^2 = 0.87$ , slope = 0.32), with the linearity spanning the full range of measurements (Figure 4a). This indicates that the optical measurements of BrC are indeed a good BB tracer.

**Table 3.** Spearman correlation between optical measurements of carbonaceous aerosols ~~Brown Carbon~~brown carbon (BrC) and ~~Black Carbon~~black carbon (eBC) and selected smoke tracers levoglucosan (Lev.), galactosan (Gal.), WSOC, WSK, OC and EC measured at the Monserrate site. Correlation coefficients are shown for all data, as well as for the low and high BB seasons, respectively.  $n$  represents the number of samples.

		Lev.	Gal.	WSOC	WSK	OC	EC
All-data (n=58)	BrC	0.87	0.72	0.78	0.54	0.76	0.53
	eBC	0.35	0.36	0.53	0.41	0.60	0.97
High-BB (n=34)	BrC	0.85	0.70	0.75	0.46	0.69	0.38
	eBC	0.23	0.40	0.52	0.39	0.61	0.96
Low-BB (n=24)	BrC	0.66	0.60	0.34	0.13	0.52	0.88
	eBC	0.51	0.45	0.31	0.13	0.35	0.78



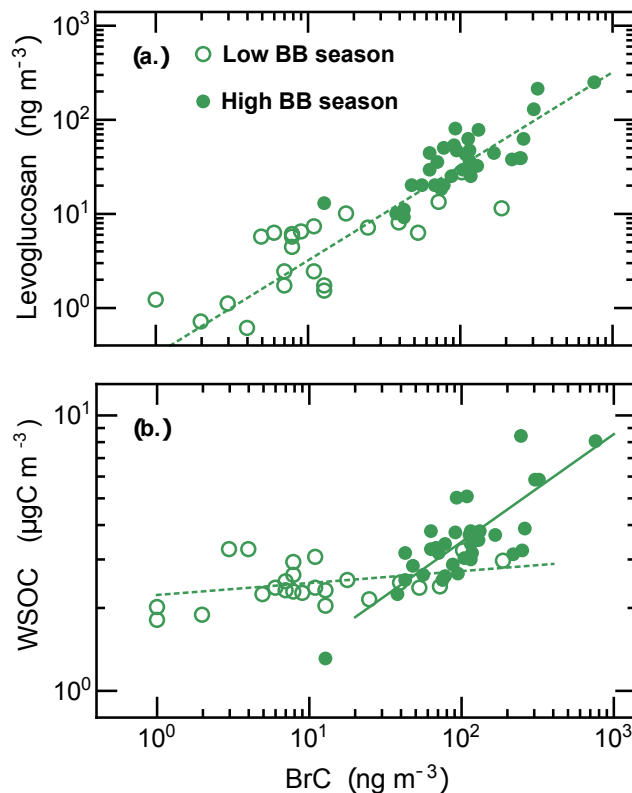


**Figure 4.** Scatter plot of daily-mean concentration of (a.) Levoglucosan and ~~Brown Carbon~~BrC, and (b.) WSOC and ~~Brown Carbon~~BrC, measured at the *Monserrate* site. Filled circles are samples collected during the high BB activity seasons, and open circles were collected during low BB activity.

Similarly strong associations were established for WSOC and other tracers (Table 3). When the association analysis is repeated only for data collected during the low-BB activity season (i.e., Campaign 2) the degree of association between BrC and WSOC drops significantly to just 0.34. This indicates that during low-BB activity months (JJA) WSOC has local sources likely not associated to BB. This is further supported by the much stronger association between levoglucosan and WSOC during high-BB seasons (0.73) compared to low-BB season (0.38). WSOC remained ~~relatively constant at values~~ between 2 and 3  $\mu\text{gC m}^{-3}$ , ~~independent of BrC concentration,~~ during the low-BB activity season (Figure 4b), ~~but increases more.~~ However, it was seen to increase steeply as a function of BrC for the high-BB activity season. ~~These observations suggest there are~~ The mean WSOC observed for low BB activity was 2.5  $\mu\text{gC m}^{-3}$  of WSOC not related to BB, and that during the while for high-BB season WSOC can reach up to activity period was 4.2  $\mu\text{gC m}^{-3}$  reaching a maximum daily-mean of to 8  $\mu\text{gC m}^{-3}$ .

The observed levoglucosan concentrations are relatively low compared to what has been observed in other studies (~~Hecobian et al., 2010~~) (e.g., ~~Hecobian et al., 2010~~). However, the measured concentration of BB tracers are significant considering the distance between the measurement site and the source regions (see Supplementary Material).

## 4 Conclusions

365 In this study we determine for the first time the presence of medium-range transported biomass burning aerosols to urban  
areas in Northern South America by direct measurement of biomass burning tracers. The presence of BB burning affected air  
masses was confirmed by multi-wavelength optical measurements of ~~Brown Carbon and Black Carbon~~brown carbon and black  
carbon, and by high-sensitivity detection of specific smoke tracers levoglucosan and galactosan. Continuous Brown Carbon  
measurements were performed during a three-year period with hourly time-resolution. These long-term observations allowed  
370 for the characterization of annual patterns in Black Carbon and Brown Carbon concentrations at the measurement site.

Despite the close proximity of the measurement site to the city center of a large, relatively polluted urban area, the statistical  
association between BrC and MODIS Active Fire data was strong on a daily basis. Furthermore, the association between BrC  
and fire counts was stronger for distant fires, i.e., those further than 400 km from the measurement site. This finding strongly  
supports the regional origin of the BB aerosol detected at the site. A source footprint analysis involving remotely sensed  
375 Fire Radiative Power data, back-trajectories calculations, and observed BrC concentration, further suggests that the eastern  
grasslands are the main biomass burning source region in NSA actually impacting populated urban areas. Our observations  
show that the annual pattern of Brown Carbon at the monitoring site was observed to have a single peak during February and  
March, coinciding with the peak in biomass burning activity in the region.

High-sensitivity levoglucosan, galactosan, and potassium measurements collocated with optical Brown Carbon observations  
380 were highly linearly correlated and showed excellent agreement. Therefore, the on-line optical observations at the measurement  
site were shown to be accurate tracers of BB aerosols when compared with well-established analytical methods. Water-soluble  
organic carbon (WSOC) was measured during high and low BB activity seasons. These observations suggest there are  $2.5$   
 $\mu\text{gC m}^{-3}$  of WSOC not related to BB, and that BB can contribute to WSOC, at which time can reach up to  $8 \mu\text{gC m}^{-3}$  for a  
24 hour period.

385 The findings of this work demonstrate that background aerosol levels are increased every year due to the presence of aged  
biomass burning aerosols. The observed Brown Carbon and smoke tracer concentrations increase in close relation to the  
amount of MODIS detected fires. Despite the overwhelming black carbon signal coming from traffic emissions, a clear relation  
between the Brown Carbon signal and regional biomass burning aerosols is established. This results highlight that even distant  
biomass burning sources resulting from uncontrolled agricultural burns and deforestation negatively impact air quality in  
390 densely populated areas hundreds of kilometers away, and that they do so in a regular basis. During our observation period, the  
~~maximum monthly mean contribution of Brown Carbon~~month with the largest contribution of BB aerosols to light-absorbing  
material was ~~13%~~13% in March with  $10\% \pm 5\%$ . The month with the largest load of BB aerosols was February of 2019, with  
 $15\% \pm 6\%$ . The uncertainty estimates in this fraction are due to uncertainty on the assumed absorption Angstrom exponent for  
biomass burning and fossil fuel burning used in the attribution algorithm.

395 *Data availability.* The data used in this article is available and will be provided upon request.

*Author contributions.* Conceptualization: R.M.B. and L.C.B., Investigation: J.M.R, M.A.R., M.Q.A. and A.P.S. Methodology: R.M.B., J.F.M. and A.P.S. Writing - Original Draft: J.M.R and R.M.B. Writing - review and editing: A.P.S., J.F.M. and L.C.B. Visualization: R.M.B., J.M.R. and M.A.R.

*Competing interests.* The authors declare that they have no conflict of interest.

400 *Acknowledgements.* This study was funded by the Colombian *Administrative Department of Science, Technology and Innovation - COL-CIENCIAS*, project No. 1204-745-56533 under grant contract No. FP44842-050-2017, and by the FAPA program from the Office of the vice-dean for Research from Universidad de los Andes. The authors thank the *Sanctuary of Monserrate* administration for kindly allowing the display of measurement devices and for providing sustained logistic support throughout the measurement period.

## References

- 405 Akagi, S. K., Yokelson, R. J., Wiedinmyer, C., Alvarado, M. J., Reid, J. S., Karl, T., Crounse, J. D., and Wennberg, P. O.: Emission factors for open and domestic biomass burning for use in atmospheric models, *Atmos. Chem. Phys.*, 11, 4039–4072, <https://doi.org/10.5194/acp-11-4039-2011>, <https://www.atmos-chem-phys.net/11/4039/2011/>, 2011.
- [Andreae, M. O. and Gelencsér, A.: Black carbon or brown carbon? The nature of light-absorbing carbonaceous aerosols, \*Atmos. Chem. Phys.\*, 6, 3131–3148, <https://doi.org/10.5194/acp-6-3131-2006>, <https://www.atmos-chem-phys.net/6/3131/2006/>, 2006.](https://doi.org/10.5194/acp-6-3131-2006)
- 410 Aurell, J. and Gullett, B. K.: Emission Factors from Aerial and Ground Measurements of Field and Laboratory Forest Burns in the Southeastern U.S.: PM<sub>2.5</sub>, Black and Brown Carbon, VOC, and PCDD/PCDF, *Environ. Sci. Technol.*, 47, 8443–8452, <https://doi.org/10.1021/es402101k>, <http://pubs.acs.org/doi/abs/10.1021/es402101k>, 2013.
- Birch, M. E. and Cary, R. A.: Elemental Carbon-Based Method for Monitoring Occupational Exposures to Particulate Diesel Exhaust, *Aerosol Sci. Tech.*, 25, 221–241, <https://doi.org/10.1080/02786829608965393>, 1996.
- 415 Bond, T. C., Streets, D. G., Yarber, K. F., Nelson, S. M., Woo, J.-H., and Klimont, Z.: A technology-based global inventory of black and organic carbon emissions from combustion, *Journal of Geophysical Research: Atmospheres*, 109, <https://doi.org/10.1029/2003JD003697>, <https://agupubs.onlinelibrary.wiley.com/doi/abs/10.1029/2003JD003697>, 2004.
- Bond, T. C., Doherty, S. J., Fahey, D. W., Forster, P. M., Berntsen, T., DeAngelo, B. J., Flanner, M. G., Ghan, S., Kärcher, B., Koch, D., Kinne, S., Kondo, Y., Quinn, P. K., Sarofim, M. C., Schultz, M. G., Schulz, M., Venkataraman, C., Zhang, H., Zhang, S., Bellouin, N., Guttikunda, S. K., Hopke, P. K., Jacobson, M. Z., Kaiser, J. W., Klimont, Z., Lohmann, U., Schwarz, J. P., Shindell, D., Storelvmo, T., Warren, S. G., and Zender, C. S.: Bounding the role of black carbon in the climate system: A scientific assessment, *J. Geophys. Res. Atmos.*, 118, 5380–5552, <https://doi.org/10.1002/jgrd.50171>, 2013.
- 420 Carslaw, D. C. and Ropkins, K.: openair - An R package for air quality data analysis, *Environ. Model. Softw.*, 27–28, 52–61, <https://doi.org/10.1016/j.envsoft.2011.09.008>, 2012.
- 425 Chen, S., Russell, L., Cappa, C., Zhang, X., Kleeman, M., Kumar, A., Liu, D., and Ramanathan, V.: Comparing black and brown carbon absorption from AERONET and surface measurements at wintertime Fresno, *Atmos. Environ.*, 199, 164–176, <https://doi.org/10.1016/j.atmosenv.2018.11.032>, <https://linkinghub.elsevier.com/retrieve/pii/S1352231018308045>, 2018.
- Cottle, P., Strawbridge, K., and McKendry, I.: Long-range transport of Siberian wildfire smoke to British Columbia: Lidar observations and air quality impacts, *Atmos. Environ.*, 90, 71–77, <https://doi.org/10.1016/j.atmosenv.2014.03.005>, 2014.
- 430 Crutzen, P. J. and Andreae, M. O.: Biomass Burning in the Tropics : Impact on Atmospheric Chemistry and Biogeochemical Cycles, *Science*, 250, 1669–1678, <https://doi.org/10.1126/science.250.4988.1669>, 1991.
- Cubison, M. J., Ortega, A. M., Hayes, P. L., Farmer, D. K., Day, D., Lechner, M. J., Brune, W. H., Apel, E., Diskin, G. S., Fisher, J. A., Fuelberg, H. E., Hecobian, A., Knapp, D. J., Mikoviny, T., Riemer, D., Sachse, G. W., Sessions, W., Weber, R. J., Weinheimer, A. J., Wisthaler, A., and Jimenez, J. L.: Effects of aging on organic aerosol from open biomass burning smoke in aircraft and laboratory studies, *Atmos. Chem. Phys.*, 11, 12 049–12 064, <https://doi.org/10.5194/acp-11-12049-2011>, <https://www.atmos-chem-phys.net/11/12049/2011/>, 2011.
- 435 de Oliveira Alves, N., Brito, J., Caumo, S., Arana, A., de Souza Hacon, S., Artaxo, P., Hillamo, R., Teinilä, K., de Medeiros, S. R. B., and de Castro Vasconcellos, P.: Biomass burning in the Amazon region: Aerosol source apportionment and associated health risk assessment, *Atmos. Environ.*, 120, 277 – 285, <https://doi.org/https://doi.org/10.1016/j.atmosenv.2015.08.059>, 2015.

- 440 Donnelly, A. A., Broderick, B. M., and Misstear, B. D.: The effect of long-range air mass transport pathways on PM10 and NO2 concentrations at urban and rural background sites in Ireland: Quantification using clustering techniques, *J. Environ. Sci. Heal. Part A*, 50, 647–658, <https://doi.org/10.1080/10934529.2015.1011955>, <http://www.tandfonline.com/doi/full/10.1080/10934529.2015.1011955>, 2015.
- Draxler, R. and Hess, G.: An Overview of the HYSPLIT\_4 Modelling System for Trajectories, Dispersion, and Deposition, *Aust. Meteorol. Mag.*, 47, 295–308, 1998.
- 445 Drinovec, L., Močnik, G., Zotter, P., Prévôt, A. S. H., Ruckstuhl, C., Coz, E., Rupakheti, M., Sciare, J., Müller, T., Wiedensohler, A., and Hansen, A. D. A.: The "dual-spot" Aethalometer: An improved measurement of aerosol black carbon with real-time loading compensation, *Atmos. Meas. Tech.*, 8, 1965–1979, <https://doi.org/10.5194/amt-8-1965-2015>, <https://www.atmos-meas-tech.net/8/1965/2015/>, 2015.
- Forster, C., Wandinger, U., Wotawa, G., James, P., Mattis, I., Althausen, D., Simmonds, P., O'Doherty, S., Jennings, S. G., Kleefeld, C., Schneider, J., Trickl, T., Kreipl, S., Jäger, H., and Stohl, A.: Transport of boreal forest fire emissions from Canada to Europe, *J. Geophys. Res.*, 106, 22 887–22 906, <https://doi.org/10.1029/2001JD900115>, 2001.
- 450 Garcia-Hurtado, E., Pey, J., Borrás, E., Sánchez, P., Vera, T., Carratalá, A., Alastuey, A., Querol, X., and Vallejo, V. R.: Atmospheric PM and volatile organic compounds released from Mediterranean shrubland wildfires, *Atmos. Environ.*, 89, 85–92, <https://doi.org/10.1016/j.atmosenv.2014.02.016>, 2014.
- Gonçalves, C., Figueiredo, B. R., Alves, C. A., Cardoso, A. A., Da Silva, R., Kanzawa, S. H., and Vicente, A. M.: Chemical characterisation of total suspended particulate matter from a remote area in Amazonia, *Atmos. Res.*, 182, 102–113, <https://doi.org/10.1016/J.ATMOSRES.2016.07.027>, <http://www.sciencedirect.com/ezproxy.uniandes.edu.co:8080/science/article/pii/S0169809516302071>, 2016.
- 455 Haikerwal, A., Akram, M., Del Monaco, A., Smith, K., Sim, M. R., Meyer, M., Tonkin, A. M., Abramson, M. J., and Dennekamp, M.: Impact of Fine Particulate Matter (PM2.5) Exposure During Wildfires on Cardiovascular Health Outcomes., *J. Am. Heart Assoc.*, 4, e001 653, <https://doi.org/10.1161/JAHA.114.001653>, <http://www.ncbi.nlm.nih.gov/pubmed/26178402><http://www.pubmedcentral.nih.gov/articlerender.fcgi?artid=PMC4608063>, 2015.
- 460 Hamburger, T., Matisāns, M., Tunved, P., Ström, J., Calderon, S., Hoffmann, P., Hochschild, G., Gross, J., Schmeissner, T., Wiedensohler, A., and Krejci, R.: Long-term in situ observations of biomass burning aerosol at a high altitude station in Venezuela: Sources, impacts and interannual variability, *Atmos. Chem. Phys.*, 13, 9837–9853, <https://doi.org/10.5194/acp-13-9837-2013>, <http://www.atmos-chem-phys.net/13/9837/2013/>, 2013.
- 465 Harrison, R. M., Beddows, D. C., Jones, A. M., Calvo, A., Alves, C., and Pio, C.: An evaluation of some issues regarding the use of Aethalometers to measure woodsmoke concentrations, *Atmos. Environ.*, 80, 540 – 548, <https://doi.org/https://doi.org/10.1016/j.atmosenv.2013.08.026>, 2013.
- Hecobian, A., Zhang, X., Zheng, M., Frank, N., Edgerton, E. S., and Weber, R. J.: Water-Soluble Organic Aerosol material and the light-absorption characteristics of aqueous extracts measured over the Southeastern United States, *Atmos. Chem. Phys.*, 10, 5965–5977, <https://doi.org/10.5194/acp-10-5965-2010>, <https://www.atmos-chem-phys.net/10/5965/2010/>, 2010.
- 470 Hennigan, C. J., Sullivan, A. P., Collett Jr., J. L., and Robinson, A. L.: Levoglucosan stability in biomass burning particles exposed to hydroxyl radicals, *Geophys. Res. Lett.*, 37, <https://doi.org/10.1029/2010GL043088>, 2010.
- Hernandez, A. J., Morales-Rincon, L. A., W., D., Mallia, D., Lin, J., and Jimenez, R.: Transboundary transport of biomass burning aerosols and photochemical pollution in the Orinoco River Basin", *Atmos. Environ.*, 205, 1 – 8, <https://doi.org/https://doi.org/10.1016/j.atmosenv.2019.01.051>, <http://www.sciencedirect.com/science/article/pii/S1352231019300810>, 2019.
- 475

- Janhäll, S., Andreae, M. O., and Pöschl, U.: Biomass burning aerosol emissions from vegetation fires: particle number and mass emission factors and size distributions, *Atmos. Chem. Phys.*, 10, 1427–1439, <https://doi.org/10.5194/acp-10-1427-2010>, <https://www.atmos-chem-phys.net/10/1427/2010/>, 2010.
- 480
- Jeong, C., Hopke, P., Kim, E., and Lee, D.: The comparison between thermal-optical transmittance Elemental Carbon and Aethalometer Black Carbon measured at multiple monitoring sites, *Atmos. Environ.*, 38, 5193–5204, <https://doi.org/10.1016/j.atmosenv.2004.02.065>, 2004.
- Justice, C. O., Giglio, L., Korontzi, S., Owens, J., Morisette, J. T., Roy, D., Descloitres, J., Alleaume, S., Petitcolin, F., and Kaufman, Y.: The MODIS fire products, *Remote Sens. Environ.*, 83, 244–262, [https://doi.org/10.1016/S0034-4257\(02\)00076-7](https://doi.org/10.1016/S0034-4257(02)00076-7), 2002.
- 485
- Kirchstetter, T. W., Novakov, T., and Hobbs, P. V.: Evidence that the spectral dependence of light absorption by aerosols is affected by organic carbon, ~~*Geophysical Research, J. Geophys. Res.*~~, 109, 1–12, <https://doi.org/10.1029/2004JD004999>, <https://agupubs.onlinelibrary.wiley.com/doi/abs/10.1029/2004JD004999>, 2004.
- Koch, D., Bond, T. C., Streets, D., Unger, N., and van der Werf, G. R.: Global impacts of aerosols from particular source regions and sectors, *J. Geophys. Res.*, 112, D02 205, <https://doi.org/10.1029/2005JD007024>, <http://doi.wiley.com/10.1029/2005JD007024>, 2007.
- 490
- Kollanus, V., Tiittanen, P., Niemi, J. V., and Lanki, T.: Effects of long-range transported air pollution from vegetation fires on daily mortality and hospital admissions in the Helsinki metropolitan area, Finland, *Environ. Res.*, 151, 351–358, <https://doi.org/10.1016/J.ENVRES.2016.08.003>, <http://www.sciencedirect.com/science/article/pii/S001393511630353X?via%3Dihub>, 2016.
- 495
- Lack, D. A. and Langridge, J. M.: On the attribution of black and brown carbon light absorption using the Ångström exponent, *Atmos. Chem. Phys.*, 13, 10535–10543, <https://doi.org/10.5194/acp-13-10535-2013>, <https://www.atmos-chem-phys.net/13/10535/2013/>, 2013.
- Lack, D. A., Bahreini, R., Langridge, J. M., Gilman, J. B., and Middlebrook, A. M.: Brown carbon absorption linked to organic mass tracers in biomass burning particles, *Atmos. Chem. Phys.*, 13, 2415–2422, <https://doi.org/10.5194/acp-13-2415-2013>, <https://www.atmos-chem-phys.net/13/2415/2013/>, 2013.
- 500
- Laskin, A., Laskin, J., and Nizkorodov, S. A.: Chemistry of Atmospheric Brown Carbon, *Chemical Reviews*, 115, 4335–4382, <https://doi.org/10.1021/cr5006167>, 2015.
- Marengo, J. A., Tomasella, J., Alves, L. M., Soares, W. R., and Rodriguez, D. A.: The drought of 2010 in the context of historical droughts in the Amazon region, *Geophysical Research Letters*, 38, <https://doi.org/10.1029/2011GL047436>, <https://agupubs.onlinelibrary.wiley.com/doi/abs/10.1029/2011GL047436>, 2011.
- 505
- Martinsson, J., Azeem, H. A., Sporre, M. K., Bergström, R., Ahlberg, E., and Öström, E.: Carbonaceous Aerosol Source Apportionment Using the Aethalometer Model – evaluation by radiocarbon and levoglucosan analysis at a rural background site in southern Sweden, *Atmos. Chem. Phys.*, 17, 4265–4281, 2017.
- Massabò, D., Caponi, L., Bernardoni, V., Bove, M., Brotto, P., Calzolari, G., Cassola, F., Chiari, M., Fedi, M., Fermo, P., Giannoni, M., Lucarelli, F., Nava, S., Piazzalunga, A., Valli, G., Vecchi, R., and Prati, P.: Multi-wavelength optical determination of black and brown carbon in atmospheric aerosols, *Atmos. Environ.*, 108, 1 – 12, <https://doi.org/https://doi.org/10.1016/j.atmosenv.2015.02.058>, <http://www.sciencedirect.com/science/article/pii/S1352231015001831>, 2015.
- 510
- Mendez-Espinosa, J., Belalcazar, L., and Morales Betancourt, R.: Regional Air Quality Impact of Northern South America Biomass Burning Emissions, *Atmos. Environ.*, 203, 131 – 140, <https://doi.org/https://doi.org/10.1016/j.atmosenv.2019.01.042>, <http://www.sciencedirect.com/science/article/pii/S135223101930072X>, 2019.
- 515

- [Mkoma, S. L., Kawamura, K., and Fu, P. Q.: Contributions of biomass/biofuel burning to organic aerosols and particulate matter in Tanzania, East Africa, based on analyses of ionic species, organic and elemental carbon, levoglucosan and mannosan, Atmos. Chem. Phys., 13, 10325–10338, https://doi.org/10.5194/acp-13-10325-2013, 2013.](https://doi.org/10.5194/acp-13-10325-2013)
- 520 Pachón, J. E., Weber, R. J., Zhang, X., Mulholland, J. A., and Russell, A. G.: Revising the use of potassium (K) in the source apportionment of PM<sub>2.5</sub>, Atmospheric Pollution Research, 4, 14 – 21, <https://doi.org/10.5094/APR.2013.002>, <http://www.sciencedirect.com/science/article/pii/S1309104215303962>, 2013.
- Pachón, J. E., Galvis, B., Lombana, O., Carmona, L. G., Fajardo, S., Rincón, A., Meneses, S., Chaparro, R., Nedbor-Gross, R., and Henderson, B.: Development and Evaluation of a Comprehensive Atmospheric Emission Inventory for Air Quality Modeling in the Megacity of Bogotá, Atmosphere, 9, <https://doi.org/10.3390/atmos9020049>, <http://www.mdpi.com/2073-4433/9/2/49>, 2018.
- 525 Petzold, A., Ogren, J. A., Fiebig, M., Laj, P., Li, S.-M., Baltensperger, U., Holzer-Popp, T., Kinne, S., Pappalardo, G., Sugimoto, N., Wehrli, C., Wiedensohler, A., and Zhang, X.-Y.: Recommendations for reporting "black carbon" measurements, Atmos. Chem. Phys., 13, 8365–8379, <https://doi.org/10.5194/acp-13-8365-2013>, <https://www.atmos-chem-phys.net/13/8365/2013/>, 2013.
- Phuleria, H. C., Fine, P. M., Zhu, Y. F., and Sioutas, C.: Air quality impacts of the October 2003 Southern California wildfires, J. Geophys. Res., 110, D07S20–D07S20, <https://doi.org/10.1029/2004JD004626>, <http://onlinelibrary.wiley.com/doi/10.1029/2004JD004626/full>, 530 2005.
- Poveda, G., Waylen, P. R., and Pulwarty, R. S.: Annual and inter-annual variability of the present climate in northern South America and southern Mesoamerica, Palaeogeography, Palaeoclimatology, Palaeoecology, 234, 3 – 27, <https://doi.org/10.1016/j.palaeo.2005.10.031>, late Quaternary climates of tropical America and adjacent seas, 2006.
- Prenni, A. J., Demott, P. J., Sullivan, A. P., Sullivan, R. C., Kreidenweis, S. M., and Rogers, D. C.: Biomass burning as a 535 potential source for atmospheric ice nuclei: Western wildfires and prescribed burns, Geophysical Research Letters, 39, 1–5, <https://doi.org/10.1029/2012GL051915>, 2012.
- Pulwarty, R. S., Barry, R. G., Hurst, C. M., Sellinger, K., and Mogollon, L. E.: Meteorology , and Atmospheric Physics Precipitation in the Venezuelan Andes in the Context of Regional Climate, Meteorology and Atmospheric Physics, 237, 217–237, 1998.
- Reid, C. E., Jerrett, M., Tager, I. B., Petersen, M. L., Mann, J. K., and Balmes, J. R.: Differential respiratory health effects from the 540 northern California wildfires: A spatiotemporal approach, Environ. Res., 150, 227–235, <https://doi.org/10.1016/J.ENVRES.2016.06.012>, <http://www.sciencedirect.com.ezproxy.uniandes.edu.co:8080/science/article/pii/S001393511630247X?via%7B%7D3Dihub>, 2016.
- Sandradewi, J., Prévot, A. S. H., Szidat, S., Perron, N., Alfarra, M. R., Lanz, V. A., Weingartner, E., and Baltensperger, U.: Using Aerosol Light Absorption Measurements for the Quantitative Determination of Wood Burning and Traffic Emission Contributions to Particulate Matter, Environmental Science & Technology, 42, 3316–3323, <https://doi.org/10.1021/es702253m>, <https://doi.org/10.1021/es702253m>, pMID: 18522112, 2008.
- 545 [Saturno, J., Holanda, B. A., Pöhlker, C., Ditas, F., Wang, Q., Moran-Zuloaga, D., Brito, J., Carbone, S., Cheng, Y., Chi, X., Ditas, J., Hoffmann, T., Hrabě de Angelis, I., Könemann, T., Lavrič, J. V., Ma, N., Ming, J., Paulsen, H., Pöhlker, M. L., Rizzo, L. V., Schlag, P., Su, H., Walter, D., Wolff, S., Zhang, Y., Artaxo, P., Pöschl, U., and Andreae, M. O.: Black and brown carbon over central Amazonia: long-term aerosol measurements at the ATTO site, Atmospheric Chemistry and Physics, 18, 12817–12843, <https://doi.org/10.5194/acp-18-12817-2018>, <https://www.atmos-chem-phys.net/18/12817/2018/>, 2018.](https://doi.org/10.5194/acp-18-12817-2018)
- Schmeissner, T., Krejci, R., Ström, J., Birmili, W., Wiedensohler, A., Hochschild, G., Gross, J., Hoffmann, P., and Calderon, S.: Analysis of number size distributions of tropical free tropospheric aerosol particles observed at Pico Espejo (4765 m a.s.l.), Venezuela, Atmos. Chem. Phys., 11, 3319–3332, <https://doi.org/10.5194/acp-11-3319-2011>, <https://www.atmos-chem-phys.net/11/3319/2011/>, 2011.

- Shen, Z., Zhang, Q., Cao, J., Zhang, L., Lei, Y., Huang, Y., Huang, R., Gao, J., Zhao, Z., Zhu, C., Xiuli, Y., Zheng, C., Xu, H.,  
555 and Liu, S.: Optical properties and possible sources of brown carbon in PM<sub>2.5</sub> over Xian, China, *Atmos. Environ.*, 150, 322–330,  
<https://doi.org/10.1016/j.atmosenv.2016.11.024>, <http://dx.doi.org/10.1016/j.atmosenv.2016.11.024>, 2017.
- Simoneit, B., Schauer, J., Nolte, C., Oros, D., Elias, V., Fraser, M., Rogge, W., and Cass, G.: Levoglucosan, a tracer for cellulose in biomass  
burning and atmospheric particles, *Atmos. Environ.*, 33, 173 – 182, [https://doi.org/https://doi.org/10.1016/S1352-2310\(98\)00145-9](https://doi.org/https://doi.org/10.1016/S1352-2310(98)00145-9), 1999.
- Stein, A. F., Draxler, R. R., Rolph, G. D., Stunder, B. J., Cohen, M. D., and Ngan, F.: NOAA’s HYSPLIT atmospheric transport and dispersion  
560 modeling system, *Bull. Am. Meteorol.*, 96, 2059–2077, <https://doi.org/10.1175/BAMS-D-14-00110.1>, 2015.
- Stohl, A., Aamaas, B., Amann, M., Baker, L. H., Bellouin, N., Berntsen, T. K., Boucher, O., Cherian, R., Collins, W., Daskalakis, N.,  
Dusinska, M., Eckhardt, S., Fuglestedt, J. S., Harju, M., Heyes, C., Hodnebrog, Hao, J., Im, U., Kanakidou, M., Klimont, Z., Kupiainen,  
K., Law, K. S., Lund, M. T., Maas, R., MacIntosh, C. R., Myhre, G., Myriokefalitakis, S., Olivie, D., Quaas, J., Quennehen, B., Raut, J. C.,  
Rumbold, S. T., Samset, B. H., Schulz, M., Seland, Shine, K. P., Skeie, R. B., Wang, S., Yttri, K. E., and Zhu, T.: Evaluating the climate  
565 and air quality impacts of short-lived pollutants, *Atmos. Chem. Phys.*, 15, 10 529–10 566, <https://doi.org/10.5194/acp-15-10529-2015>,  
2015.
- Su, L., Yuan, Z., Fung, J. C., and Lau, A. K.: A comparison of HYSPLIT backward trajectories generated from two GDAS datasets, *Sci.  
Total Environ.*, 506-507, 527–537, <https://doi.org/10.1016/J.SCITOTENV.2014.11.072>, 2015.
- Sullivan, A. P. and Weber, R. J.: Chemical characterization of the ambient organic aerosol soluble in water: 1. Isolation of hydrophobic and  
570 hydrophilic fractions with a XAD-8 resin, *J. Geophys. Res.*, 111, <https://doi.org/10.1029/2005JD006485>, 2006a.
- Sullivan, A. P. and Weber, R. J.: Chemical characterization of the ambient organic aerosol soluble in water: 2. Isolation of acid, neutral, and  
basic fractions by modified size-exclusion chromatography, *J. Geophys. Res.*, 111, <https://doi.org/10.1029/2005JD006486>, 2006b.
- Sullivan, A. P., Holden, A. S., Patterson, L. A., McMeeking, G. R., Kreidenweis, S. M., Malm, W. C., Hao, W. M., Wold, C. E., and  
Collett Jr., J. L.: A method for smoke marker measurements and its potential application for determining the contribution of biomass  
575 burning from wildfires and prescribed fires to ambient PM<sub>2.5</sub> organic carbon, *Journal of Geophysical Research: Atmospheres*, 113,  
<https://doi.org/10.1029/2008JD010216>, 2008.
- Sullivan, A. P., Frank, N., Kenski, D. M., and Collett, J. L.: Application of high-performance anion-exchange chromatography-pulsed am-  
perometric detection for measuring carbohydrates in routine daily filter samples collected by a national network: 1 Determination of the  
impact of biomass burning in the upper Midwest, *J. Geophys. Res.*, 116, <https://doi.org/10.1029/2010JD014169>, 2011.
- 580 Thornhill, G. D., Ryder, C. L., Highwood, E. J., Shaffrey, L. C., and Johnson, B. T.: The Effect of South American Biomass Burn-  
ing Aerosol Emissions on the Regional Climate, *Atmos. Chem. Phys. Discuss.*, pp. 1–34, <https://doi.org/10.5194/acp-2017-953>,  
<https://www.atmos-chem-phys-discuss.net/acp-2017-953/>, 2017.
- Tsimpidi, A. P., Karydis, V. A., Pandis, S. N., and Lelieveld, J.: Global combustion sources of organic aerosols: model  
comparison with 84 AMS factor-analysis data sets, *Atmos. Chem. Phys.*, 16, 8939–8962, <https://doi.org/10.5194/acp-16-8939-2016>, 2016.
- 585 Tzompa-Sosa, Z. A., Sullivan, A. P., Retama, A., and Kreidenweis, S. M.: Contribution of Biomass Burning to Carbonaceous Aerosols in  
Mexico City during May 2013, *Aerosol and Air Quality Research*, 16, 114–124, <https://doi.org/10.4209/aaqr.2015.01.0030>, 2016.
- van der Werf, G. R., Randerson, J. T., Giglio, L., Collatz, G. J., Mu, M., Kasibhatla, P. S., Morton, D. C., DeFries, R. S., Jin, Y., and van  
Leeuwen, T. T.: Global fire emissions and the contribution of deforestation, savanna, forest, agricultural, and peat fires (1997–2009),  
*Atmos. Chem. Phys.*, 10, 11 707–11 735, <https://doi.org/10.5194/acp-10-11707-2010>, <https://www.atmos-chem-phys.net/10/11707/2010/>,  
590 2010.



- Virkkula, A., Mäkelä, T., Hillamo, R., Yli-Tuomi, T., Hirsikko, A., Hämeri, K., and Koponen, I.: A Simple Procedure for Correcting Loading Effects of Aethalometer Data, *J. Air & Waste Manage. Assoc.*, 57, 1214–1222, <https://doi.org/10.3155/1047-3289.57.10.1214>, 2007.
- Wang, J., Nie, W., Cheng, Y., Shen, Y., Chi, X., Wang, J., Huang, X., Xie, Y., Sun, P., Xu, Z., Qi, X., Su, H., and Ding, A.: Light absorption of brown carbon in eastern China based on 3-year multi-wavelength aerosol optical property observations and an improved absorption Ångström exponent segregation method, *Atmos. Chem. Phys.*, 18, 9061–9074, <https://doi.org/10.5194/acp-18-9061-2018>, 2018.
- 595 Weber, R. J., Sullivan, A. P., Peltier, R. E., Russell, A., Yan, B., Zheng, M., de Gouw, J., Warneke, C., Brock, C., Holloway, J. S., Atlas, E. L., and Edgerton, E.: A study of secondary organic aerosol formation in the anthropogenic-influenced southeastern United States, *J. Geophys. Res.*, 112, <https://doi.org/10.1029/2007JD008408>, 2007.
- Wong, J. P., Tsagkaraki, M., Tsiodra, I., Mihalopoulos, N., Violaki, K., Kanakidou, M., Sciare, J., Nenes, A., and Weber, R. J.: Effects of Atmospheric Processing on the Oxidative Potential of Biomass Burning Organic Aerosols, *Environmental Science & Technology*, 53, 6747–6756, <https://doi.org/10.1021/acs.est.9b01034>, <https://doi.org/10.1021/acs.est.9b01034>, PMID: 31091086, 2019.
- 600 Yamasoe, M. A., Artaxo, P., Miguel, A. H., and Allen, A. G.: Chemical composition of aerosol particles from direct emissions of vegetation fires in the Amazon Basin: water-soluble species and trace elements, *Atmos. Environ.*, 34, 1641 – 1653, [https://doi.org/https://doi.org/10.1016/S1352-2310\(99\)00329-5](https://doi.org/https://doi.org/10.1016/S1352-2310(99)00329-5), 2000.
- 605 [Yan, C., Zheng, M., Bosch, C., Andersson, A., Desyaterik, Y., A.P. S., Collett, J., Zhao, B., Wang, S., He, K., and Gustagsson, O.: Important fossil source contribution to brown carbon in Beijing during winter. \*Scientific Reports\*, 7, <https://doi.org/10.1038/srep43182>, 2017.](https://doi.org/10.1038/srep43182)
- Youssef, H., Liousse, C., Roblou, L., Assamoi, E. M., Salonen, R. O., Maesano, C., Banerjee, S., and Annesi-Maesano, I.: Quantifying wildfires exposure for investigating health-related effects, <https://doi.org/10.1016/j.atmosenv.2014.07.041>, 2014.